A 3D spatial channel model for cellular radio.

Sasiakos, Christos.

Monterey, California. Naval Postgraduate School

NAVAL POSTGRADUATE SCHOOL
Monterey, California

THESIS

A 3D SPATIAL CHANNEL MODEL FOR CELLULAR RADIO

by

Christos Sasiakos

September 2000

Thesis Advisor: Ramakrishna Janaswamy
Second Reader: Tri T. Ha

Approved for public release; distribution is unlimited

REPORT DOCUMENTATION PAGE			Form Approved OMB No. 0704-0188
Public reporting burden for this collection of information is estimated to average 1 hour per response, including the time for reviewing instruction, searching existing data sources, gathering and maintaining the data needed, and completing and reviewing the collection of information. Send comments regarding this burden estimate or any other aspect of this collection of information, including suggestions for reducing this burden, to Washington headquarters Services, Directorate for Information Operations and Reports, 1215 Jefferson Davis Highway, Suite 1204, Arlington, VA 22202-4302, and to the Office of Management and Budget, Paperwork Reduction Project (0704-0188) Washington DC 20503.			
1. AGENCY USE ONLY *(Leave blank)*	**2. REPORT DATE** September 2000	**3. REPORT TYPE AND DATES COVERED** Master's Thesis	
4. TITLE AND SUBTITLE: A 3D Spatial Channel model for cellular radio.			**5. FUNDING NUMBERS**
6. AUTHOR(S) Christos Sasiakos			
7. PERFORMING ORGANIZATION NAME(S) AND ADDRESS(ES) Naval Postgraduate School Monterey, CA 93943-5000			**8. PERFORMING ORGANIZATION REPORT NUMBER**
9. SPONSORING / MONITORING AGENCY NAME(S) AND ADDRESS(ES)			**10. SPONSORING / MONITORING AGENCY REPORT NUMBER**
11. SUPPLEMENTARY NOTES The views expressed in this thesis are those of the author and do not reflect the official policy or position of the Department of Defense or the U.S. Government.			
12a. DISTRIBUTION / AVAILABILITY STATEMENT Approved for public release; distribution is unlimited			**12b. DISTRIBUTION CODE**

13. ABSTRACT ***(maximum 200 words)***

This thesis provides closed form expressions for the angular distribution in azimuth and elevation planes for a geometrically based single bounce spheroid model. The geometry of the spheroid is defined by the semi-major axis a and the semi-minor axis b. The other parameter of interest in the model is the distance D between the base station and the mobile station. The latter is assumed to be at the center of the spheroid. The mobile station is assumed to be the transmitter, while the base station is the receiver. This thesis investigates the effects of the above parameters on the angular distribution of the received waves. Important parameters such as the r.m.s angle spread in azimuth and elevation plane are calculated from the p.d.f. expressions derived. The behaviour of these r.m.s angle spreads versus the ratio a/D or b/D respectively is also investigated.

14. SUBJECT TERMS Spatial channel Model, Joint TOA/AOA pdf, AOA Marginal pdf in Azimuth Plane, AOA Marginal pdf in Elevation Plane, r.m.s angle spread			**15. NUMBER OF PAGES** 68
			16. PRICE CODE
17. SECURITY CLASSIFICATION OF REPORT Unclassified	**18. SECURITY CLASSIFICATION OF THIS PAGE** Unclassified	**19. SECURITY CLASSIFICATION OF ABSTRACT** Unclassified	**20. LIMITATION OF ABSTRACT** UL

NSN 7540-01-280-5500

Standard Form 298 (Rev. 2-89)
Prescribed by ANSI Std. 239-18

THIS PAGE INTENTIONALLY LEFT BLANK

Approved for public release; distribution is unlimited

A 3D SPATIAL CHANNEL MODEL FOR CELLULAR RADIO

Christos Sasiakos
Lieutenant, Hellenic Navy
B.S.E.E. , Hellenic Naval Academy, 1988

Submitted in partial fulfillment of the
requirements for the degree of

MASTER OF SCIENCE IN ELECTRICAL ENGINEERING

from the

NAVAL POSTGRADUATE SCHOOL
September 2000

ABSTRACT

This thesis provides closed form expressions for the angular distribution in azimuth and elevation planes for a geometrically based single bounce spheroid model. The geometry of the spheroid is defined by the semi-major axis a and the semi-minor axis b. The other parameter of interest in the model is the distance D between the base station and the mobile station. The latter is assumed to be at the center of the spheroid. The mobile station is assumed to be the transmitter, while the base station is the receiver. This thesis investigates the effects of the above parameters on the angular distribution of the received waves. Important parameters such as the r.m.s angle spread in azimuth and elevation plane are calculated from the p.d.f. expressions derived. The behaviour of these r.m.s angle spreads versus the ratio a/D or b/D respectively is also investigated.

THIS PAGE INTENTIONALLY LEFT BLANK

TABLE OF CONTENTS

EXECUTIVE SUMMARY

This thesis provides closed forms which describe the statistics of the angular distribution in azimuth and elevation planes for geometrically based single bounce spheroid model. This spatial model can be generated by revolving an ellipse, which lies on the xz plane of a 3D Cartesian coordinate system, about the x-axis. This ellipse has semi-major axis a and semi-minor axis b, respectively. The base and the mobile stations are located in the xy plane with the mobile station being at the center of the spheroid and the base station at the origin of the coordinate system. It is assumed that the mobile station is transmitting and the base station is receiving. The base and mobile stations are separated by a distance D.

The scattering spheroid model is applicable to a macrocell environment in which the received multipath signals at the base station are originated after a scattering from the surrounding environment about the mobile station. Assuming that the scatterers are uniformly distributed with a constant scatterer density function in the volume V as defined by the geometry of the spheroid, we derive the marginal angle of arrival (AOA) probability density functions (p.d.f). in the azimuth and elevation plane.

Using the derived closed forms for both p.d.f.s we generate plots to examine how the parameters a, b and D affect the angular distribution of the received waves. From the marginal AOA p.d.f. in the azimuth plane we conclude that:

1. The higher the ratio *a/D*, the lower the probability for the received multipath signals at the base station to be confined to a small angular region centered about the axis which connects the base and the mobile stations.

2. The angular distribution in the azimuth plane is independent of the length of the vertical dimension *b* of the spheroid.

3. Comparing the results of the spheroid model for small values of *b* with those of the circular scattering model presented in [Ref. 3], it was observed that there exists a significant difference between them.

Additionally, the effect of the *a/D* ratio on the r.m.s angle spread in azimuth plane is discussed. From the plot results of the r.m.s angle spread in azimuth plane versus *a/D*, we conclude that for values of *a/D* up to 0.5, there exists a linear relation. However, for higher values of *a/D*, the relationship changes to a nonlinear curve with a positive gradient.

Regarding the marginal AOA p.d.f. in the elevation plane, the following conclusions were drawn from the plots:

1. Similar to the p.d.f in the azimuth plane, the higher the ratio *b/D* the lower the probability for the received multipath components at the base station to be restricted in a small angular spread around the axis, which connects the base and the mobile stations.

2. The r.m.s angle spread which also depends on the semi major axis *a*, has a linear dependence with respect to the *b/D* ratio.

AKNOWLEDGMENT

The author would like to thank Prof. R.Janaswamy for his support and his guidance through every step of this thesis, my wife, Maria, for all her patience, and understanding.

THIS PAGE INTENTIONALLY LEFT BLANK

I. INTRODUCTION

A. BACKGROUND

The outdoor radio environment contains a large number of obstacles, such as buildings, cars, hills, etc, which obstruct, reflect and scatter the wireless radio signals. As a result, the transmitted signal arrives at the mobile station or at the base station from many different angles and times of arrival; this is known as multipath. Another common phenomenon in cellular systems is the co-channel interference, and it is created because in a certain geographic region(cluster) there are other subregions(cells) that utilize the same set of frequencies. Multipath fading and co-channel interference can increase significantly the bit error rate and they don't allow high bit rate data services in wireless communications systems. The presence of multipath and the motion of the receiver or the transmitter causes the received signal envelope to be time-varying and experience a Doppler shift that depends upon the angle of arrival of the incoming waves. Concepts such as angular spread, time delay spread, and Doppler spread have to be taken in consideration during a wireless communication system evaluation. In particular, they should be taken into consideration in the design of smart antennas used for diversity, beamforming and emitter localization applications.

The multipath effect alone can be countered by applying antenna spatial diversity which implements an antenna array consisting of multi-elements. Spatial diversity is an arrangement whereby signals from multiple elements are combined to result in a signal that fades less rapidly than the individual element signals. Ideally this can be

accomplished if received signals at the two elements are decorrelated. The degree of the decorrelation between the two received signals by the two elements can be expressed by the spatial cross-correlation coefficient which is a function of the joint p.d.f. $f_{\phi,\theta}(\phi,\theta)$ describing the angular distribution of the incoming waves in the three-dimensional space at the receiver.

The interference limited factor can not be overcome by using spatial diversity. Switched beam arrays can be used with some success if the angle of arrival of the interfering signal is not near the angle of arrival of the desired signal [Ref. 1]. Only the beamforming arrays have the potential to completely suppress the co-channel interference (if the number of elements exceeds the number of co-channel interferers) improving the wireless communication system performance. The performance of these type of smart antennas depends on the spatial characteristics of the wireless radio channel. The term "spatial characteristics of the radio channel" is used to mean the statistics of the received signal envelope in the spatial domain. These spatial characteristics may not always be available from measurements. In such a case one needs to devise geometric models to depict the scattering process in the spatial domain. Another area where knowledge of angular distribution is valuable is in the determination of the power spectral density [Ref. 1]. Therefore the angular distribution of the received multipath components is important in evaluating the performance of radiowave link between the transmitter and the receiver in wireless communications.

Spatial channel models have been created and applied in order to be able to derive the statistics of the received signal envelope for both macrocell and microcell environments. The term macrocell enviroment assumes that the scatterers surrounding the mobile station have the same height or are higher than the antenna of the mobile. This results in a received signal at the mobile station which arrives from all directions after bouncing from the surrounding scatterers. In contrast, the base station's antenna is located higher than the surrounding scatterers. Therefore the received multipath signals at the base station originate after scattering from the area near to the mobile station [Ref.2]. In microcell enviroment both base and mobile station are deployed in the same height as the surrounding scatterers. This implies that the scattering process takes place near to the base and mobile station. The characteristic difference between the types of environments is that the angular spread of the received signals at the base station is confined to a small region for macrocell environments. In the microcell enviroment this region tends to be larger.

In Table 1, which is a modified version of a table from [Ref 2.], are listed some representative spatial channel models.

SPATIAL CHANNEL MODEL	DESCRIPTION OF THE MODEL	APPLICATIONS
1. Lee's Model	Scatterers are evenly spaced on a circular ring about the mobile at a distance R. Each of the scatterrers represents the effect of many other scatterers and hence is referred to as an effective scatterer. The base station is deployed a distance D from the mobile station.	Predicts correlation coefficient using a discrete angle of arrival(AOA) model. A modified version of this model can account for a Doppler shift, assuming that the scatterers are moving with an angular velocity.
2. Discrete Uniform Distribution	A model similar to Lee's model with the N scatterers evenly spaced over an AOA range.	Predicts correlation coefficient using a discrete AOA model. The correlation predicted by this model falls off more quickly than the correlation in Lee's model.
3. Geometrically Based Circular Model	In this model it is assumed that the scatterers are uniformly deployed within a radius R about the mobile. The locations of the scatterers are defined by a spatial scatterer density function.	It is suitable for macrocell environments and predicts the joint time of arrival(TOA) and AOA and marginal density functions at both base station and mobile station.
4. Geommetrically Based Elliptical Model	Scatterers are uniformly distributed in an ellipse where the base station and mobile station are the focii of the ellipse.	It can be determined the marginal AOA, TOA, the joint TOA and AOA density function. It is applied in microcell enviroment.
5. Gaussian Wide Sense Stationery Uncorrellated Scattering (GWSSUS)	N scatterers are grouped into clusters in space such that the delay differences within each cluster are not resolvable within the transmission signal BW.	Provides an analytical model for the array covariance matrix.

6. Gaussian Angle of Arrival (GAA)	Special case of the GWSSUS model with a single cluster and angle of arrival statistics assumed to be Gaussian distributed about some nominal angle.	Provides an analytical model for the array covariance matrix.

Table 1. Description of some representative spatial channel models. "From Ref. [2]."

Figure 1 through 4 demonstrate the first four spatial channel models, listed in Table 1.

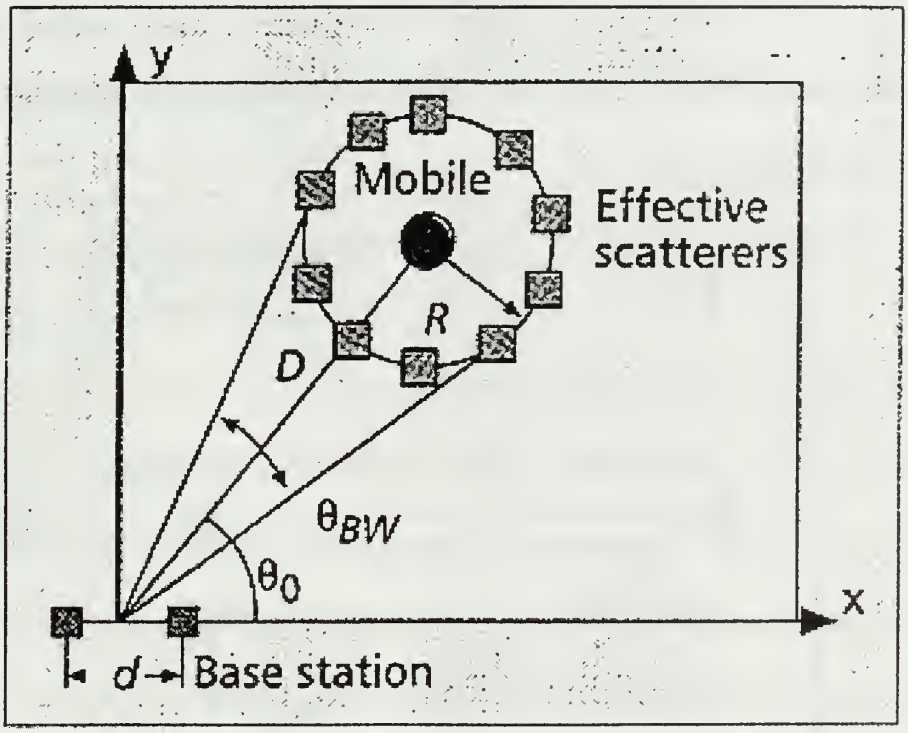

Figure 1. Lee's Model "From Ref. [2]."

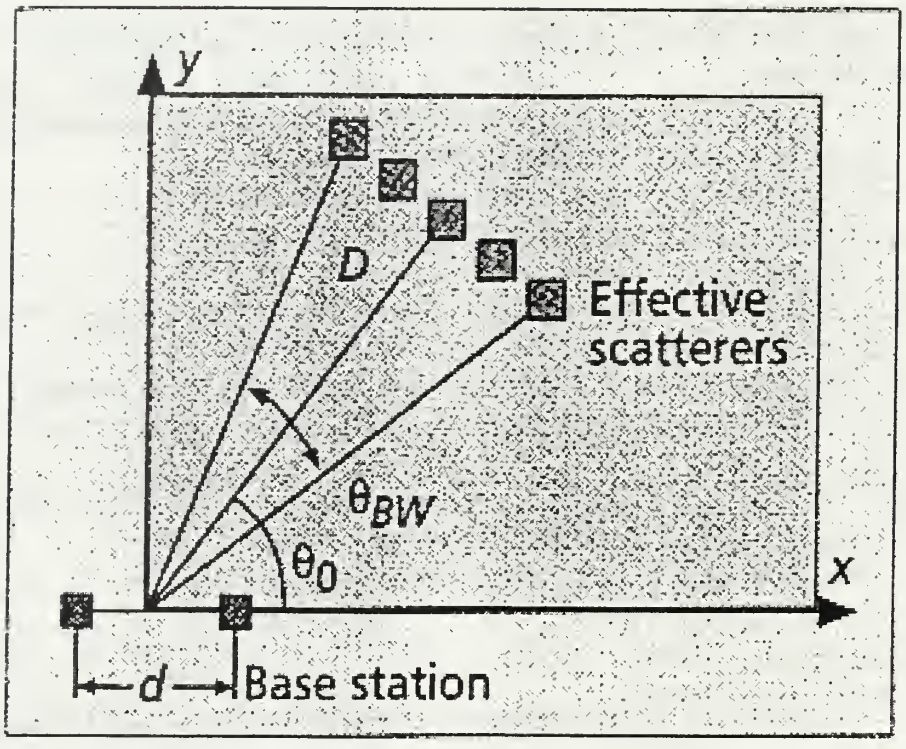

Figure 2. Discrete Uniform Distribution Model "From Ref. [2]".

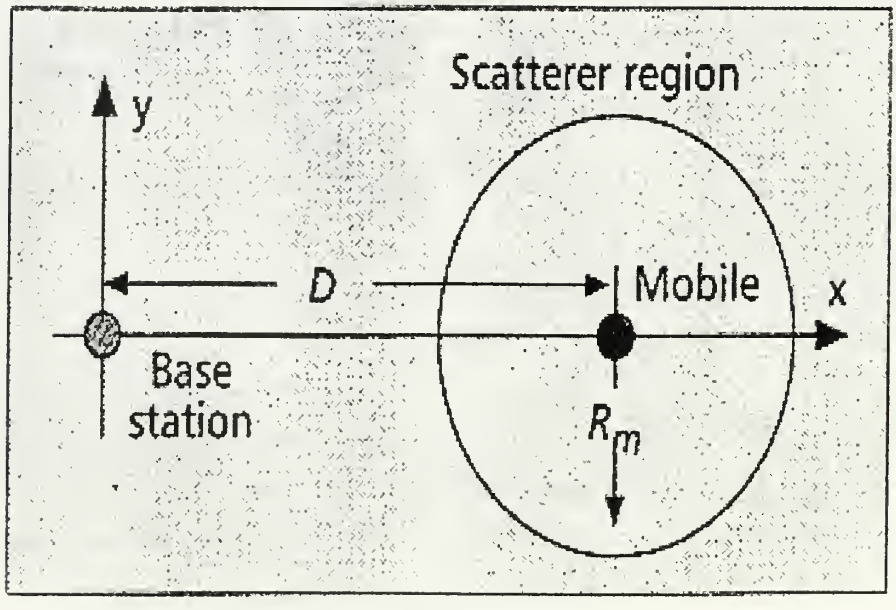

Figure 3. Geommetrically Based Circular Model "From Ref.[2]".

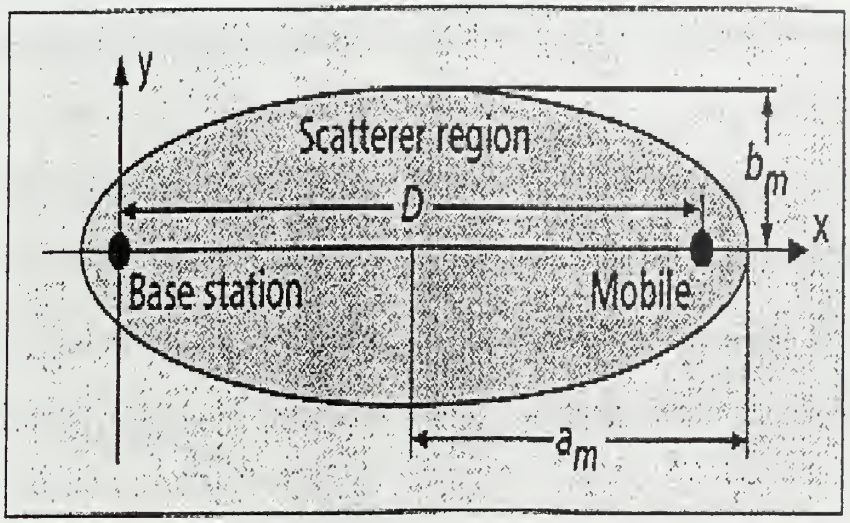

Figure 4. Geommetrically Based Elliptical Model From Ref.[2]".

Every spatial channel listed in Table 1 has one common feature; the received signal at the base station is assumed to arrive from a two dimensional plane connecting the tips of the transmitter and the receiver. Hence the angle of arrival (AOA) includes only the azimuth angle information.

In this thesis we consider a 3D spheroid model as shown in Figure 5 This spheroid can be generated by revolving an ellipse, which lies on xz plane, with semi-major axis and semi-minor axis a and b, respectively, about the x-axis. The base station and the mobile station are located in the xy plane with the mobile station at the center of the spheroid, and the base station at the origin. It is assumed that the mobile station is transmitting and the base station is receiving. The distance between the two terminals is D with the requirement that the semi-major axis of the spheroid be less than or equal to

the distance D. In the model considered here it is obvious that the angle of arrival (AOA) of the received signals includes both the azimuth and elevation plane coordinates.

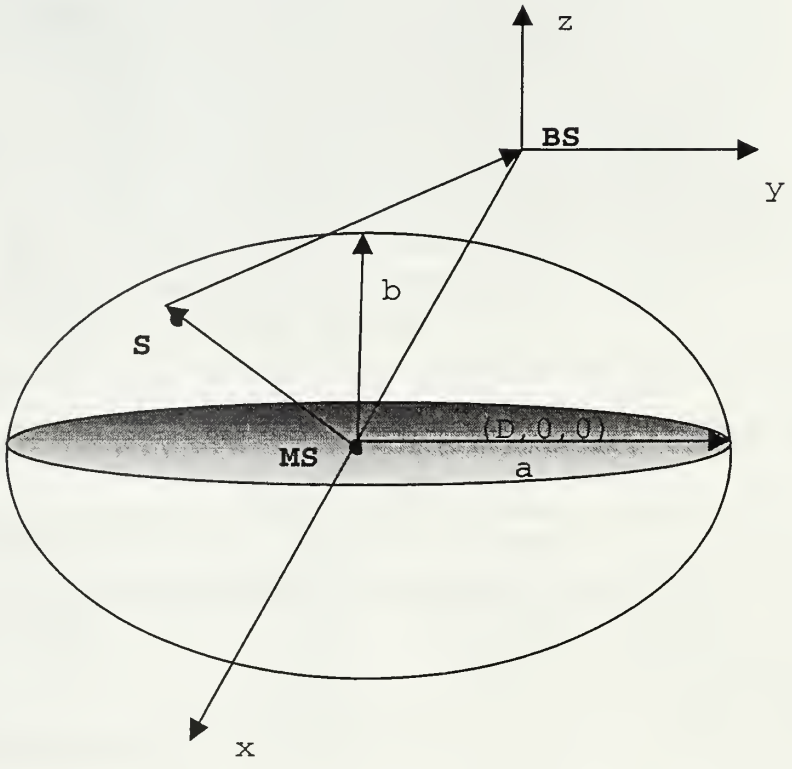

Figure 5. The spheroid geometry.

B. OBJECTIVE

Assuming that the scatterers are uniformly distributed around the mobile station as defined by the geometry of the spheroid, the objective is to derive the marginal probability density function (p.d.f.) angles of arrival (AOA) in the azimuth and in the elevation planes at the base station. After extracting these quantities, we investigate how the angular spread in azimuth and elevation plane are related with the dimensions of the spheroid and the distance between the transmitter and the receiver, as well as how they are correlated with each other.

THIS PAGE INTENTIONALLY LEFT BLANK

II. PROBLEM FORMULATION

A. INTRODUCTION

In this chapter we consider a single bounce scattering spheroid model. The model can be used in a macrocell environment where the base station antenna height is relatively high. As a result there will be no scattering from scatterers near the base station. Figure 6, shows the spheroid scatterer density geometry and the notation used to derive the marginal p.d.f.s. As is shown in the Figure 6, the location of each scatterer is defined by the Cartesian coordinates (x, y, z) or the spherical coordinates (r_b, ϕ_b, θ_b), or (r_b, ϕ_b, β), where β represents the complementary angle of θ_b in elevation plane.

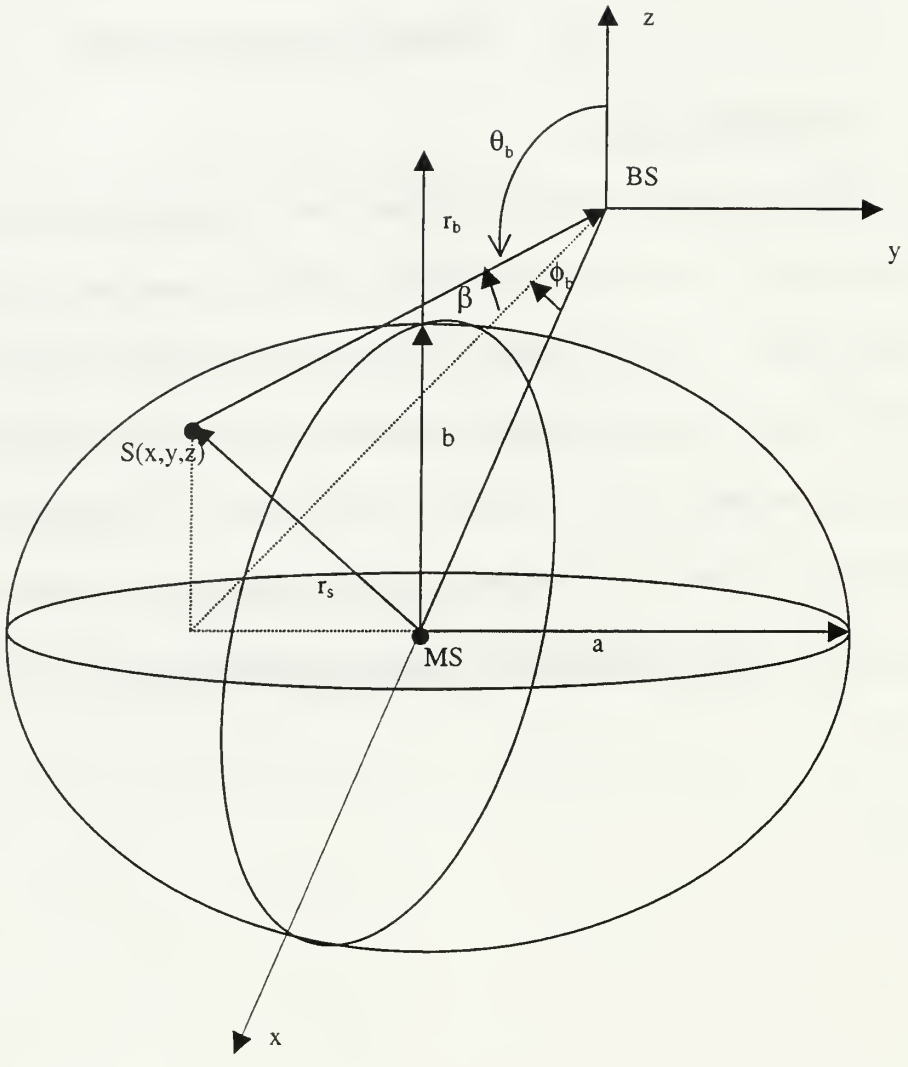

Figure 6. The spheroid scatterer density geometry.

The method for the derivation of the joint TOA/AOA p.d.f. and marginal AOA p.d.f. for both azimuth and elevation planes is based on the approach presented in [Ref. 3]. In the Figure 6, it is assumed that scatterers are distributed randomly in the volume V of the spheroid according to the spatial scatterer density function $f_{x,y,z}(x,y,z)$. It is further assumed that the waves arrive directly at the base station after undergoing scattering only

once from within the volume V. Multiple scattering of waves is not considered in this thesis.

Before proceeding with the determination of the p.d.f.s in the azimuth and the elevation plane we would like to present the formulation for the joint TOA/AOA p.d.f and marginal AOA p.d.f in the general case. In section B we start with the derivation of the joint TOA/AOA p.d.f.. In section C, we show formulation for the marginal AOA p.d.f.s. In the following sections D through G we derive the marginal AOA p.d.f in azimuth and elevation plane for the spheroidal model.

B. DERIVATION OF THE JOINT TOA/AOA P.D.F.'S

Figure 7, shows a plane wave impinging on a base station after scattering from an obstacle, represented by a point 'S' in space with the ordered rectangular triples (x, y, z).

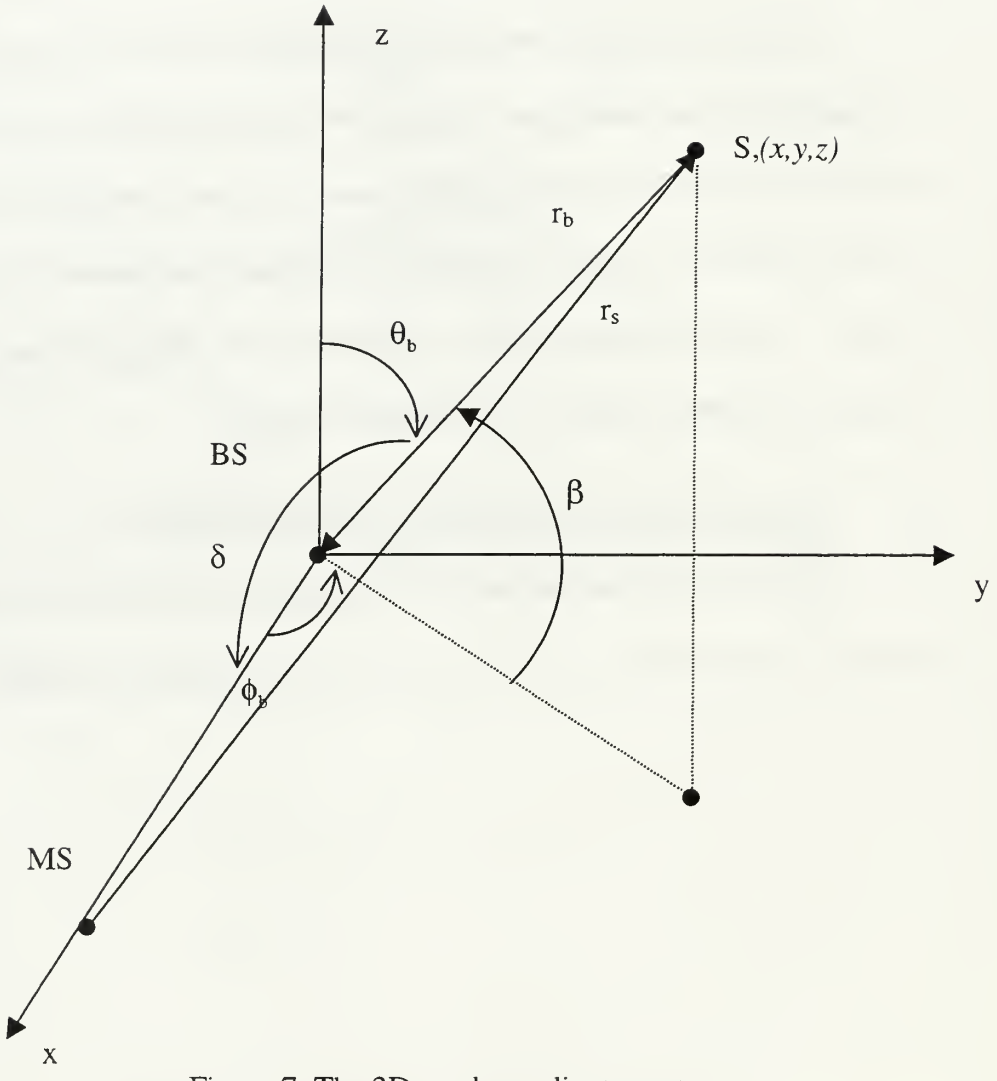

Figure 7. The 3D used coordinate system.

The scatterer probability density function $f_{x,y,z}(x,y,z)$ can be also expressed terms of spherical coordinates systems (r_b, ϕ_b, θ_b) as follows. The equations relating the spherical coordinates to the Cartesian coordinates are:

$$r_b = \sqrt{x^2 + y^2 + z^2} \tag{1}$$

$$\theta_b = \cos^{-1}\left(\frac{z}{\sqrt{x^2+y^2+z^2}}\right) \tag{2}$$

$$\phi_b = \tan^{-1}(\frac{y}{x}) \tag{3}$$

$$x = r_b \sin\theta_b \cos\phi_b \tag{4}$$

$$y = r_b \sin\theta_b \sin\phi_b \tag{5}$$

$$z = r_b \cos\theta_b \tag{6}$$

where (x, y, z) and (r_b, ϕ_b, θ_b) denote the location of the scatterer in Cartesian and spherical coordinates respectively. The joint p.d.f $f_{r_b,\phi_b,\theta_b}(r_b, \phi_b, \theta_b)$ can be found using the well known transformation [Ref. 4]:

$$f_{r_b,\phi_b,\theta_b}(r_b, \phi_b, \theta_b) = J(r_b, \phi_b, \theta_b) f_{x,y,z}(x, y, z)\Big|_{\substack{x = r_b \sin\theta_b \cos\phi_b \\ y = r_b \sin\theta_b \sin\phi_b \\ z = r_b \cos\theta_b}} \tag{7}$$

where $J(r_b, \phi_b, \theta_b)$ is the determinant of the Jacobian transformation given by:

$$J(r_b, \phi_b, \theta_b) = \begin{vmatrix} \frac{\partial x}{\partial r_b} & \frac{\partial x}{\partial \phi_b} & \frac{\partial x}{\partial \theta_b} \\ \frac{\partial y}{\partial r_b} & \frac{\partial y}{\partial \phi_b} & \frac{\partial y}{\partial \theta_b} \\ \frac{\partial z}{\partial r_b} & \frac{\partial z}{\partial \phi_b} & \frac{\partial z}{\partial \theta_b} \end{vmatrix} = r_b^2 \sin\theta_b, \qquad 0 < \theta_b < \pi \tag{8}$$

Substituting the equation (8) into (7) we get for the scatterer probability density function $f_{r_b,\phi_b,\theta_b}(r_b, \phi_b, \theta_b)$ with respect to spherical coordinates:

$$f_{r_b,\phi_b,\theta_b}(r_b, \phi_b, \theta_b) = r_b^2 \sin\theta_b f_{x,y,z}(r_b \sin\theta_b \cos\phi_b, r_b \sin\theta_b \sin\phi_b, r_b \cos\theta_b). \tag{9}$$

If we want to express the scatterer probability density function $f_{r_b,\phi_b,\theta_b}(r_b, \phi_b, \theta_b)$ with respect to (τ, ϕ_b, θ_b), where τ denotes the time delay of the multipath component, we have first to find the relationship between r_b and the τ. Applying the law of cosines to the triangle BS,S,MS we get the following equation:

$$r_s^2 = r_b^2 + D^2 - 2r_b D\cos\delta \tag{10}$$

where the $\cos\delta$ is called the 'cosine direction' given by:

$$\cos\delta = \sin\theta_b \cos\phi_b . \tag{11}$$

The delay corresponding to the total path traveled by the wave is:

$$\tau = \frac{r_b + r_s}{c} = \frac{1}{c}\left(r_b + \sqrt{r_b^2 + D^2 + 2r_b D\sin\theta_b \cos\phi_b}\right) \tag{12}$$

where 'c' is the speed of propagation of waves.

Squaring both sides of the equation (12) and solving for r_b gives:

$$r_b = \frac{D^2 - \tau^2 c^2}{2(D\sin\theta_b \cos\phi_b - \tau c)} \tag{13}$$

The joint TOA/AOA p.d.f. $f_{\tau,\phi_b,\theta_b}(\tau,\phi_b,\theta_b)$ can be found using the Jacobian transformation [Ref. 4] according to:

$$f_{\tau,\phi_b,\theta_b}(\tau,\phi_b,\theta_b) = \frac{f_{r_b,\phi_b,\theta_b}(r_b,\phi_b,\theta_b)}{|J(r_b,\phi_b,\theta_b)|}\Bigg|_{r_b = \frac{D^2-\tau^2c^2}{2(D\sin\theta_b\cos\phi_b - \tau c)}} \tag{14}$$

where $|J(r_b,\phi_b,\theta_b)|$ is the determinant of the Jacobian tranformation given by:

$$|J(r_b,\phi_b,\theta_b)| = \left|\frac{\partial r_b}{\partial \tau}\right|^{-1} = \frac{2(D\sin\theta_b\cos\phi_b - \tau c)^2}{D^2 c + \tau^2 c^3 - 2\tau c^3 D\sin\theta_b\cos\phi_b} . \tag{15}$$

Substituting the equation (15) into (14) we get for the joint TOA/AOA p.d.f. $f_{\tau,\phi_b,\theta_b}(\tau,\phi_b,\theta_b)$

$$f_{\tau,\phi_b,\theta_b}(\tau,\phi_b,\theta_b) = \frac{D^2 c + \tau^2 c^3 - 2\tau c^2 D\sin\theta_b\cos\phi_b}{2(D\sin\theta_b\cdot\cos\phi_b - \tau c)^2} f_{r_b,\phi_b,\theta_b}\left(\frac{D^2-\tau^2c^2}{2(D\sin\theta_b\cos\phi_b - \tau c)},\phi_b,\theta_b\right). \tag{16}$$

Using the last equation (16) and the equations (9) and (13) we can express the joint TOA/AOA p.d.f. $f_{\tau,\phi_b,\theta_b}(\tau,\phi_b,\theta_b)$ in terms of original scatterer probability density function $f_{x,y,z}(x,y,z)$ as follows:

$$f_{\tau,\phi_b,\theta_b}(\tau,\phi_b,\theta_b) = \sin\theta_b \frac{(D^2-\tau^2c^2)^2(D^2c+\tau^2c^3-2\tau c^2 D\sin\theta_b\cos\phi_b)}{8(D\sin\theta_b\cos\phi_b-\tau c)^4} f_{x,y,z}(r_b\sin\theta_b\cos\phi_b, r_b\sin\theta_b\sin\phi_b, r_b\cos\theta_b).$$

(17)

Note that the equation (17) expresses the joint TOA/AOA p.d.f. $f_{\tau,\phi_b,\theta_b}(\tau,\phi_b,\theta_b)$ as observed at the base station in terms of an arbitary scatterer probability density function $f_{x,y,z}(x,y,z)$.

When the scatterers are uniformly distributed within an arbitrarily space A with a volume V, then the scatterer probability density function $f_{x,y,z}(x,y,z)$ is given by:

$$f_{x,y,z}(x,y,z) = \begin{cases} \frac{1}{V}, x,y,z \in A \\ 0, otherwise \end{cases}. \tag{18}$$

If we consider this special case, the joint TOA/AOA p.d.f. $f_{\tau,\phi_b,\theta_b}(\tau,\phi_b,\theta_b)$ can be written:

$$f_{\tau,\phi_b,\theta_b}(\tau,\phi_b,\theta_b) = \sin\theta_b \frac{(D^2-\tau^2c^2)^2(D^2c+\tau^2c^3-2\tau c^2 D\sin\theta_b\cos\phi_b)}{8V(D\sin\theta_b\cos\phi_b-\tau c)^4} \tag{19}$$

where the range for the values of τ,ϕ_b,θ_b has to be defined.

C. DERIVATION OF MARGINAL AOA PROBABILITY DENSITY FUNCTION

The marginal AOA p.d.f. with respect to spherical angle coordinates could be found by integrating the joint p.d.f. $f_{r_b,\phi_b,\theta_b}(r_b,\phi_b,\theta_b)$, as given in equation (9) with respect to r_b over the range $r_{b_1}(\phi_b,\theta_b)$ to $r_{b_2}(\phi_b,\theta_b)$, and then either with respect to $\theta_b(\phi_b)$ over the range $\theta_{b_1}(\phi_b)$ to $\theta_{b_2}(\phi_b)$ or with respect $\phi_b(\theta_b)$ over the range $\phi_{b_1}(\theta_b)$ to $\phi_{b_2}(\theta_b)$ depending on whether the marginal A.O.A p.d.f. is to be found in

azimuth or elevation plane respectively. The terms $r_{b_1}(\phi_b,\theta_b)$ and $r_{b_2}(\phi_b,\theta_b)$ are the lower and the upper limits of integration and depend on the azimuth angle ϕ_b and the elevation angle θ_b. The values of these limits can be found from the intersections of a straight line $\theta_b = \text{constant}$, $\phi_b = \text{constant}$ with the scatterer volume. The limits of integration in θ_b, θ_{b1} and θ_{b2} for the marginal AOA p.d.f. in azimuth plane can be defined as the smallest and the largest θ_b-values that bound a region R, which is the intersection between a plane at a specific ϕ_b value and the scatterer region volume. The above statement can be expressed in mathematical expressions as follows.

The marginal AOA p.d.f. $f_{\phi_b}(\phi_b)$ in azimuth plane is given by:

$$f_{\phi_b}(\phi_b) = \int_{\theta_{b_1}(\phi_b)}^{\theta_{b_2}(\phi_b)} \int_{r_{b_1}(\phi_b,\theta_b)}^{r_{b_2}(\phi_b,\theta_b)} f_{r_b,\phi_b,\theta_b}(r_b,\phi_b,\theta_b)\,dr_b\,d\theta_b =$$

$$\int_{\theta_{b_1}(\phi_b)}^{\theta_{b_2}(\phi_b)} \int_{r_{b_1}(\phi_b,\theta_b)}^{r_{b_2}(\phi_b,\theta_b)} r_b^2 \sin\theta_b\, f_{x,y,z}(r_b\sin\theta_b\cos\phi_b, r_b\sin\theta_b\sin\phi_b, r_b\cos\theta_b)\,dr_b\,d\theta_b \,. \qquad (20)$$

The marginal AOA p.d.f. $f_{\theta_b}(\theta_b)$ in elevation plane is given by:

$$f_{\theta_b}(\theta_b) = \int_{\phi_{b_1}(\theta_b)}^{\phi_{b_2}(\theta_b)} \int_{r_{b_1}(\phi_b,\theta_b)}^{r_{b_2}(\phi_b,\theta_b)} f_{r_b,\phi_b,\theta_b}(r_b,\phi_b,\theta_b)\,dr_b\,d\phi_b =$$

$$\int_{\phi_{b_1}(\theta_b)}^{\phi_{b_2}(\theta_b)} \int_{r_{b_1}(\phi_b,\theta_b)}^{r_{b_2}(\phi_b,\theta_b)} r_b^2 \sin\theta_b\, f_{x,y,z}(r_b\sin\theta_b\cos\phi_b, r_b\sin\theta_b\sin\phi_b, r_b\cos\theta_b)\,dr_b\,d\phi_b \,. \qquad (21)$$

The limits for ϕ_b integration, which depend on the elevation angle θ_b, can be determined from the smallest and the largest azimuth angles that bound the region of intersection between the cone $\theta_b = \text{constant}$ and the scatterer volume.

Equations (20) and (21) express the AOA marginal p.d.f.'s for any scatterer probability density function $f_{x,y,z}(x,y,z)$. When the scatterers are uniformly distributed in a volume with a constant probability density function $f_{x,y,z}(x,y,z)$, the marginal AOA p.d.f. $f_{\phi_b}(\phi_b)$ is given by:

$$f_{\phi_b}(\phi_b) = \frac{1}{V}\int_{\theta_{b_1}(\theta_b)}^{\theta_{b_2}(\theta_b)}\int_{r_{b_1}(\phi_b,\theta_b)}^{r_{b_2}(\phi_b,\theta_b)} r_b^2 \sin\theta_b \, dr_b \, d\theta_b = \frac{1}{3V}\int_{\theta_b(\phi_b)}^{\theta_{b_2}(\phi_b)}\left[r_{b_2}^3(\phi_b,\theta_b) - r_{b_1}^3(\phi_b,\theta_b)\right]\sin\theta_b \, d\theta_b \tag{22}$$

and the marginal AOA p.d.f. $f_{\theta_b}(\theta_b)$ is given by:

$$f_{\theta_b}(\theta_b) = \frac{1}{V}\int_{\phi_{b_1}(\theta_b)}^{\phi_{b_2}(\theta_b)}\int_{r_{b_1}(\phi_b,\theta_b)}^{r_{b_2}(\phi_b,\theta_b)} r_b^2 \sin\theta_b \, dr_b \, d\phi_b = \frac{1}{3V}\int_{\phi_{b_1}(\theta_b)}^{\phi_{b_2}(\theta_b)}\left[r_{b_2}^3(\phi_b,\theta_b) - r_{b_1}^3(\phi_b,\theta_b)\right]\sin\theta_b \, d\phi_b . \tag{23}$$

D. MARGINAL AOA P.D.F. IN AZIMUTH PLANE FOR THE SPHEROID SPATIAL CHANNEL MODEL

Before we proceed to find the marginal AOA p.d.f. in the azimuth plane, we have to define the equation which describes the geometry of the spheroid in Cartesian and spherical coordinates. The spheroid in Cartesian coordinates is given by:

$$\frac{(x-D)^2+y^2}{a^2} + \frac{z^2}{b^2} = 1 \tag{24}$$

and in spherical coordinates is given by:

$$(a^2\cos^2\theta_b + b^2\sin^2\theta_b)r_b^2 - 2Db^2 r_b \sin\theta_b\cos\phi_b + b^2\left(D^2 - a^2\right) = 0 . \tag{25}$$

Instead of the polar angle θ_b, its complementary $\beta = \frac{\pi}{2} - \theta_b$ will be used hereafter for simplicity. Equation (25) can be expressed as:

$$A(\beta) r_b^2 - B(\beta) r_b \cos\phi_b + C = 0 \tag{26}$$

where, $A(\beta) = a^2 \sin^2\beta + b^2 \cos^2\beta$, $B(\beta) = 2Db^2 \cos\beta$, $C = b^2\left(D^2 - a^2\right)$ and

$\Delta(\beta) = B^2(\beta)\cos^2\phi_b - 4A(\beta)C$

$$= 4b^2\left[a^2\left(a^2 \sin^2\beta + b^2\cos^2\beta\right) - D^2a^2\sin^2\beta - D^2b^2\cos^2\beta\sin^2\phi_b\right].$$

The two roots of the above equation are:

$$\left.\begin{aligned} r_{b_1}(\phi_b, \beta) &= \frac{Db^2\cos\beta\cos\phi_b - \sqrt{a^2b^2\left(a^2\sin^2\beta + b^2\cos^2\beta\right) - D^2b^2\left(a^2\sin^2\beta + b^2\cos^2\beta\sin^2\phi_b\right)}}{\left(a^2\sin^2\beta + b^2\cos^2\beta\right)} \\ r_{b_2}(\phi_b, \beta) &= \frac{Db^2\cos\beta\cos\phi_b + \sqrt{a^2b^2\left(a^2\sin^2\beta + b^2\cos^2\beta\right) - D^2b^2\left(a^2\sin^2\beta + b^2\cos^2\beta\sin^2\phi_b\right)}}{\left(a^2\sin^2\beta + b^2\cos^2\beta\right)} \end{aligned}\right\}. \tag{27}$$

In terms of the angle β, the marginal AOA p.d.f. $f_{\phi_b}(\phi_b)$ in azimuth plane expressed as:

$$f_{\phi_b}(\phi_b) = \frac{1}{3V}\int_{-\beta_{\max}(\phi_b)}^{\beta_{\max}(\phi_b)} \left[r_{b_2}^3(\phi_b, \beta) - r_{b_1}^3(\phi_b, \beta)\right]\cos\beta d\beta \tag{28}$$

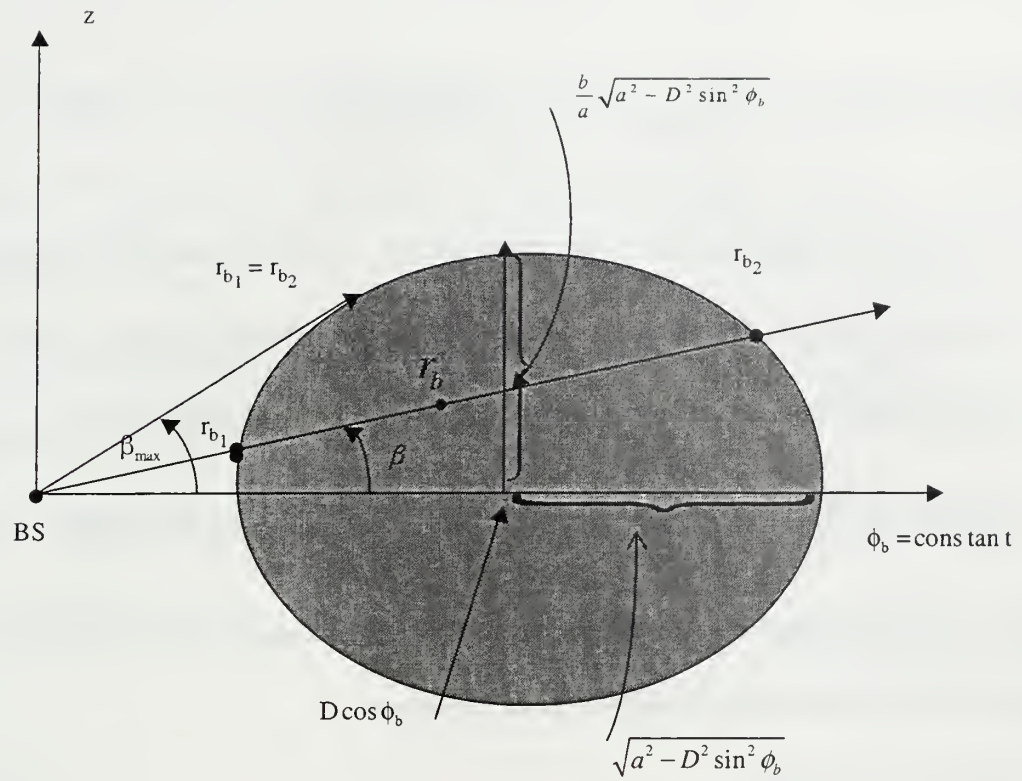

Figure 8. The intersected region R between a plane ϕ_b = constant and the spheroid.

Figure 8 shows the limits of the angle β for a specific value of ϕ_b. The limits of integration in the elevation angle can be determined from the values of the angle β that bound the region R, which is produced by the intersection between the plane ϕ_b =constant and the spheroid. In our case the cross section of the spheroid with a plane ϕ_b = constant is an ellipse with semi-major axis equals to $\sqrt{a^2 - D^2 \sin^2 \phi_b}$ and semi-minor axis equals to $\frac{b}{a}\sqrt{a^2 - D^2 \sin^2 \phi_b}$ and the center located at $D\cos\phi_b$. For a general angle β, the straight line from the origin intersects the region R at two points r_{b_1} and r_{b_2}. At the two boundary points the roots r_{b_1} and r_{b_2} of the quadratic equation (26) in r_b coincide. This happens when the discriminant of the quadratic equation is set to zero. Carrying this out, the upper limit $\beta_{\max}$ is given by:

$$\beta_{\max} = \tan^{-1}\left(\frac{b}{a}\sqrt{\frac{a^2 - D^2\cdot\sin^2\phi_b}{D^2 - a^2}}\right). \qquad (29)$$

This equation is valid for ϕ_b in the range of $\sin^{-1}\left(-\frac{a}{D}\right) \le \phi_b \le \sin^{-1}\left(\frac{a}{D}\right)$. These correspond to the values of ϕ_b that bound the spheroid in the xy-plane. Taking all of the above into consideration, the marginal AOA p.d.f. in azimuth plane is given by:

$$f_{\phi_b}(\phi_b) = \frac{2}{3V}\int_0^{\beta_{\max}(\phi_b)} \cos\beta\left[r_{b_2}^3(\phi_b,\beta) - r_{b_1}^3(\phi_b,\beta)\right]d\beta\,,\ \sin^{-1}\left(-\frac{a}{D}\right) \le \phi_b \le \sin^{-1}\left(\frac{a}{D}\right). \qquad (30)$$

The evaluation of the integral as defined in the equation (30) is straightforward. The following relations simplify some of the terms:

$$r_{b_2}^3(\phi_b,\beta) - r_{b_1}^3(\phi_b,\beta) =$$

$$= (r_{b_2}(\phi_b,\beta) - r_{b_1}(\phi_b,\beta))(r_{b_1}^2(\phi_b,\beta) + r_{b_2}(\phi_b,\beta)r_{b_1}(\phi_b,\beta) + r_{b_2}^2(\phi_b,\beta)). \qquad (31)$$

$$r_{b_2}(\phi_b,\beta) - r_{b_1}(\phi_b,\beta) = \frac{\sqrt{\Delta}}{A(\beta)} \qquad (32)$$

$$r_{b_1}(\phi_b,\beta) + r_{b_2}(\phi_b,\beta) = \frac{B(\beta)\cos\phi_b}{A(\beta)} \qquad (33)$$

$$r_{b_1}^2(\phi_b,\beta) + r_{b_2}^2(\phi_b,\beta) = \frac{B^2(\beta)\cos^2\phi_b}{A^2(\beta)} - \frac{2C}{A(\beta)} \qquad (34)$$

$$r_{b_1}(\phi_b,\beta)\cdot r_{b_2}(\phi_b,\beta) = \frac{C}{A(\beta)} \qquad (35)$$

Using equations (31) through (35) in equation (30) we get:

$$f_{\phi_b}(\phi_b) = \frac{2}{3V}\int_0^{\beta_{\max}(\phi_b)} \left(r_{b_2} - r_{b_1}\right)\left(r_{b_1}^2 + r_{b_1}r_{b_2} + r_{b_2}^2\right)\cos\beta d\beta =$$

$$= \frac{2}{3V}\int_0^{\beta_{\max}(\phi_b)} \frac{\sqrt{B^2(\beta)\cos^2\phi_b - 4A(\beta)C}}{A(\beta)}\left(\frac{B^2(\beta)\cos^2\phi_b}{A^2(\beta)} - \frac{C}{A(\beta)}\right)\cos\beta d\beta\,. \qquad (36)$$

At a specific value of ϕ_b when $\beta = \beta_{\max}$ the discriminant becomes $\Delta(\beta_{\max}) = B^2(\beta_{\max})\cos^2\phi_b - 4A(\beta_{\max})C = 0$. Hence, writing

$$\Delta(\beta) = \Delta(\beta) - \Delta(\beta_{\max})$$

$$= [B^2(\beta)\cos^2\phi_b - 4A(\beta)C] - [B^2(\beta_{\max})\cos^2\phi_b - 4A(\beta_{\max})C],$$

we see that

$$\Delta(\beta) = 4b^2\left[a^2\left(a^2\sin^2\beta + b^2\cos^2\beta\right) - D^2a^2\sin^2\beta - D^2b^2\cos^2\beta\sin^2\phi_b\right] -$$

$$-4b^2\left[a^2\left(a^2\sin^2\beta_{\max} + b^2\cos^2\beta_{\max}\right) - D^2a^2\sin^2\beta_{\max} - D^2b^2\cos^2\beta_{\max}\sin^2\phi_b\right], \tag{37}$$

which gives:

$$\Delta = 4b^2\left[\sin^2_{\beta_{\max}} - \sin^2\beta\right]\left[a^2\left(D^2 - a^2\right) + b^2\left(a^2 - D^2\sin^2\phi_b\right)\right]. \tag{38}$$

Using this the integral in equation (36) can be written as follows:

$$f_{\phi_b}(\phi_b) = \frac{16D^2b^5\cos^2\phi_b\sqrt{a^2\left(D^2-a^2\right)+b^2\left(a^2-D^2\sin^2\phi_b\right)}}{3V}\int_0^{\beta_{\max}}\frac{\cos^3\beta\sqrt{\sin^2\beta_{\max}-\sin^2\beta}}{(a^2\sin^2\beta+b^2\cos^2\beta)^3}d\beta -$$

$$-\frac{4(D^2-a^2)b^3\sqrt{a^2\left(D^2-a^2\right)+b^2\left(a^2-D^2\sin^2\phi_b\right)}}{3V}\int_0^{\beta_{\max}}\frac{\cos\beta\sqrt{\sin^2\beta_{\max}-\sin^2\beta}}{(a^2\sin^2\beta+b^2\cos^2\beta)^2}d\beta. \tag{39}$$

The first integral in equation (39) can be simplified as:

$$\int_0^{\beta_{\max}}\frac{\cos^3\beta\sqrt{\sin^2\beta_{\max}-\sin^2\beta}}{(a^2\sin^2\beta+b^2\cos^2\beta)^3}d\beta = \int_0^{\beta_{\max}}\frac{\cos\beta(1-\sin^2\beta)\sqrt{\sin^2\beta_{\max}-\sin^2\beta}}{(a^2\sin^2\beta+b^2\cos^2\beta)^3}d\beta. \tag{40}$$

On using the substitution $t = \sin\beta$, and $t_{\max} = \sin\beta_{\max}$ the last integral becomes:

$$\int_0^{\beta_{\max}}\frac{\cos\beta(1-\sin^2\beta)\sqrt{\sin^2\beta_{\max}-\sin^2\beta}}{(a^2\sin^2\beta+b^2\cos^2\beta)^3}d\beta = \int_0^{t_{\max}}\frac{\left(1-t^2\right)\sqrt{t^2_{\max}-t^2}}{\left[b^2+\left(a^2-b^2\right)t^2\right]^3}dt. \tag{41}$$

Hence the term $1-t^2$ can be written as follows:

$$1-t^2 = -\frac{1}{\left(a^2-b^2\right)}\left[-a^2+\left(b^2+\left(a^2-b^2\right)t^2\right)\right].$$

Using this in equation (41) we get:

$$\int_0^{t_{max}} \frac{\left(1-t^2\right)\sqrt{t_{max}^2-t^2}}{\left[b^2+\left(a^2-b^2\right)t^2\right]^3}dt = = \frac{a^2}{a^2-b^2}\int_0^{t_{max}} \frac{\sqrt{t_{max}^2-t^2}}{\left[b^2+\left(a^2-b^2\right)t^2\right]^3}dt - \frac{1}{a^2-b^2}\int_0^{t_{max}} \frac{\sqrt{t_{max}^2-t^2}}{\left[b^2+\left(a^2-b^2\right)t^2\right]^2}dt \tag{42}$$

Furthermore, writing $t = t_{max}\sin\alpha$, we get for the last two integrals:

$$\int_0^{t_{max}} \frac{\sqrt{t^2{}_{max}-t^2}}{\left(b^2+(a^2-b^2)t^2\right)^3}dt = \int_0^{\frac{\pi}{2}} \frac{t^2{}_{max}\cos^2\alpha}{\left(b^2+(a^2-b^2)t^2{}_{max}\sin^2\alpha\right)^3}d\alpha \tag{43}$$

and

$$\int_0^{t_{max}} \frac{\sqrt{t^2{}_{max}-t^2}}{\left(b^2+(a^2-b^2)t^2\right)^2}dt = \int_0^{\frac{\pi}{2}} \frac{t^2{}_{max}\cos^2\alpha}{\left(b^2+(a^2-b^2)t^2{}_{max}\sin^2\alpha\right)^2}d\alpha \tag{44}$$

Similarly, the second integral in equation (39) can be expressed as:

$$\int_0^{\beta_{max}} \frac{\cos\beta\sqrt{\sin^2\beta_{max}-\sin^2\beta}}{\left(b^2+(a^2-b^2)\sin^2\beta\right)^2} = \int_0^{t_{max}} \frac{\sqrt{t^2{}_{max}-t^2}}{\left(b^2+(a^2-b^2)t^2\right)^2}dt = \int_0^{\frac{\pi}{2}} \frac{t^2_{max}\cos^2\alpha}{\left(b^2+(a^2-b^2)t^2{}_{max}\sin^2\alpha\right)^2}d\alpha. \tag{45}$$

The last integrals described in the equations (43) (44) and (45) are evaluated using the formulas 2.563-1, 2.563-2, and 2.563-3 from [Ref. 5].

The marginal p.d.f. in azimuth is then given by:

$$f_{\phi_b}\left(\phi_b\right) = I_1\left(\phi_b\right) - I_2\left(\phi_b\right), \quad \sin^{-1}\left(-\frac{a}{D}\right) \le \phi_b \le \sin^{-1}\left(\frac{a}{D}\right) \tag{46}$$

where $I_1\left(\phi_b\right) = \dfrac{\pi D^2\cos^2\phi_b\sqrt{a^2\left(D^2-a^2\right)+b^2\left(a^2-D^2\sin^2\phi_b\right)}}{3V}\dfrac{\left(3a^2-4b^2\right)\gamma^2+\left(4b^4-2a^2b^2\right)\gamma-a^2b^4}{\gamma\sqrt{\gamma}\left(a^2-b^2\right)^2}$ (47)

and $I_2\left(\phi_b\right) = \dfrac{\pi(D^2-a^2)\sqrt{a^2\left(D^2-a^2\right)+b^2\left(a^2-D^2\sin^2\phi_b\right)}}{3V}\dfrac{\left(\gamma-b^2\right)}{\sqrt{\gamma}\left(a^2-b^2\right)}$, (48)

with $\gamma = a^2 \sin^2 \beta_{\max} + b^2 \cos^2 \beta_{\max}$.

E. MARGINAL AOA P.D.F IN AZIMUTH PLANE FOR THE SPECIAL CASE OF THE SEMI-MINOR AXIS OF THE SPHEROID GOING ZERO

In this section we examine the special case of marginal AOA p.d.f., given by equation (46), for values of $b \to 0$. In order to evaluate the p.d.f. for this case the following simplifications are made on equations (47) and (48):

$$\gamma = a^2 \sin^2 \beta_{\max} + b^2 \cos^2 \beta_{\max} = b^2 \cos^2 \beta_{\max} \left(1 + \frac{a^2}{b^2} \tan^2 \beta_{\max}\right)$$

where $\tan \beta_{\max}$ is given by equation (29). Since $b \to 0$ the last equation can be expressed as follows:

$$\gamma \cong \frac{b^2 D^2 \cos^2 \phi_b}{D^2 - a^2}. \tag{49}$$

The terms $\gamma - b^2$ and $(\gamma - b^2)\left(D^2 - a^2\right)$ can be expressed as:

$$\gamma - b^2 \cong b^2 \frac{a^2 - D^2 \sin^2 \phi_b}{D^2 - a^2} > 0 \text{ and } (\gamma - b^2)\left(D^2 - a^2\right) \cong b^2 \left(a^2 - D^2 \sin^2 \phi_b\right). \tag{50}$$

Plugging equations (47) and (48) to equation (46) the latter can be written as :

$$I_1(\phi_b) - I_2(\phi_b) = \frac{\pi}{3V} \frac{\sqrt{a^2\left(D^2 - a^2\right) + b^2\left(a^2 - D^2 \sin^2 \phi_b\right)}}{\sqrt{\gamma}\left(a^2 - b^2\right)}$$

$$\left\{ -\left(D^2 - a^2\right)\left(\gamma - b^2\right) + \frac{D^2 \cos^2 \phi_b}{\left(a^2 - b^2\right)} \left[\left(3a^2 - 4b^2\right)\gamma^2 + \left(4b^4 - 2a^2 b^2\right)\gamma - a^2 b^4\right]^{\frac{1}{\gamma}} \right\}. \tag{51}$$

The term $\left[\left(3a^2 - 4b^2\right)\gamma^2 + \left(4b^4 - 2a^2 b^2\right)\gamma - a^2 b^4\right]^{\frac{1}{\gamma}}$ can be expressed as:

$$\left[\left(3a^2 - 4b^2\right)\gamma^2 + \left(4b^4 - 2a^2 b^2\right)\gamma - a^2 b^4\right]^{\frac{1}{\gamma}} = 3a^2\gamma - 2a^2 b^2 - a^2 \frac{b^4}{\gamma} - 4b^2\gamma + 4b^4. \tag{52}$$

The first three terms in the right side of equation (52) are second order terms, while the last two are fourth order terms with respect to b therefore can be neglected. Hence equation (52) reduces to:

$$3a^2\gamma - 2a^2b^2 - a^2\frac{b^4}{\gamma} - 4b^2\gamma + 4b^4 \cong \frac{a^2b^2}{\left(D^2-a^2\right)}\left[3D^2\cos^2\phi_b - \left(D^2-a^2\right)\left(2+\frac{D^2-a^2}{D^2\cos^2\phi_b}\right)^2\right]. \tag{53}$$

Combining equations (49), (50) and (53) and taking also in consideration which terms are second or fourth order with respect to 'b', equation (51) can be written as follows:

$$I_1(\phi_b) - I_2(\phi_b) \cong \frac{\pi}{3V}\frac{\left(D^2-a^2\right)}{D\cos\phi_b}\frac{b}{a}\left[-a^2 + D^2\sin^2\phi_b + D^2\cos^2\phi_b\left(\frac{3D^2\cos^2\phi_b}{\left(D^2-a^2\right)} - 2 - \frac{D^2-a^2}{D^2\cos^2\phi_b}\right)\right]. \tag{54}$$

Carrying out some simplifications in equation (54) we get:

$$I_1(\phi_b) - I_2(\phi_b) = \frac{3D}{4a^3}\left(a^2 - D^2\sin^2\phi_b\right). \tag{55}$$

Finally the marginal AOA p.d.f in azimuth plane of the spheroid for the values of $b \to 0$ is given by:

$$f_{\phi_b}(\phi_b) = \frac{3D}{4a^3}\left(a^2 - D^2\sin^2\phi_b\right) \qquad \sin^{-1}\left(-\frac{a}{D}\right) \le \phi_b \le \sin^{-1}\left(\frac{a}{D}\right). \tag{56}$$

F. DERIVATION OF MARGINAL AOA PDF IN AZIMUTH PLANE THROUGH A SECOND APPROACH

As we have mentioned before the marginal AOA p.d.f in azimuth plane is given by the:

$$f_{\phi_b}(\phi_b) = \frac{1}{V}\int_{-\beta_{\max}}^{\beta_{\max}}\int_{r_{b_1}(\phi_b,\beta)}^{r_{b_2}(\phi_b,\beta)} r_b^2\sin\beta dr_b\beta = \frac{1}{V}\int_{-\beta_{\max}}^{\beta_{\max}}\int_{r_{b_1}(\phi_b,\beta)}^{r_{b_2}(\phi_b,\beta)} r_b r_b\cos\beta dr_b d\beta\,. \tag{57}$$

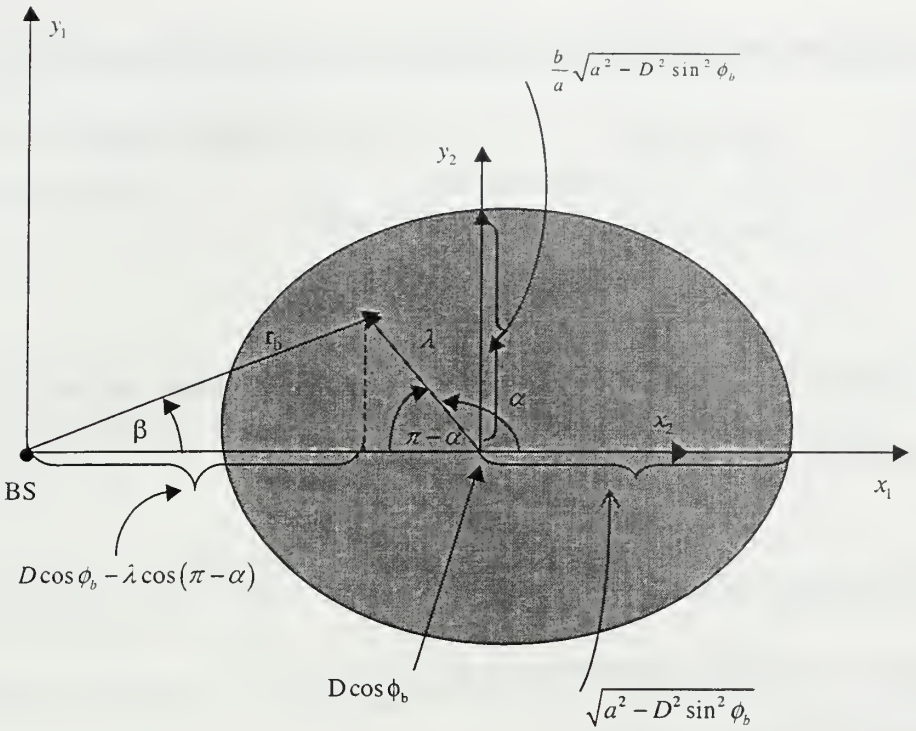

Figure 9. The 2D coordinate system used for the derivation of the azimuth p.d.f.

Figure 9, shows the intersected region between a plane at a specific ϕ_b value and the scatterer region volume. In the plane ϕ_b=constant, we adopt a 2D Cartesian coordinate system x_1y_1. The terms of the integral in the equation (57), $r_b \cos\beta$ and $r_b dr_b d\beta$ can be written as:

$$r_b \cos\beta = D\cos\phi + \lambda\cos\alpha \text{ and } r_b dr_b d\beta = dx_1 dy_1 = dx_2 dy_2 . \quad (58)$$

In the x_2y_2 2D Cartesian coordinate system as shown in Figure 9, the term $\lambda\cos\alpha = x_2$.

According to the above equation (58) equation (57) can be written as:

$$f_{\phi_b}(\phi_b) = \frac{1}{V} \int_{-\beta_{\max}}^{\beta_{\max}} \int_{r_{b_1}(\phi_b,\beta)}^{r_{b_2}(\phi_b,\beta)} r_b \cos\beta r_b dr d\beta = \frac{2}{V} \int_0^{\frac{b}{a}\sqrt{a^2 - D^2\sin^2\phi_b}} \int_0^{\sqrt{a^2 - D^2\sin^2\phi_b}} (D\cos\phi_b + \lambda\cos\alpha) dx_2 dy_2$$

(59)

The integral in equation (59) with respect to polar coordinate system λ and α can be expressed as:

$$f_{\phi_b}(\phi_b) = \frac{1}{V} \int_{\alpha=0}^{2\pi} \int_0^{\lambda_{\max}} (D\cos\phi_b + \lambda\cos\alpha)\lambda d\lambda d\alpha . \tag{60}$$

Taking in consideration that the term $\lambda\cos\alpha$ is equal to x_2, since x_2 is an odd function, equation (60) can be written as:

$$f_{\phi_b}(\phi_b) = \frac{1}{V} \int_{\alpha=0}^{2\pi} \int_0^{\lambda_{\max}} (D\cos\phi_b + x_2)\lambda d\lambda d\alpha = \frac{1}{V} \iint_{A_{\phi_b}(\phi_b)} D\cos\phi_b \lambda d\lambda d\alpha \tag{61}$$

where $A_{\phi_b}(\phi_b)$ is the area of region R.

Equation (61) is simplified as:

$$f_{\phi_b}(\phi_b) = \frac{1}{V} D\cos\phi_b \iint_{A(\phi_b)} \lambda d\lambda d\alpha = \frac{D\cos\phi_b}{V} A_{\phi_b}(\phi_b) \tag{62}$$

where $A_{\phi_b}(\phi_b) = \pi\frac{b}{a}\left(a^2 - D^2\sin^2\phi_b\right)$. Substituting the above term in equation (62) we get for the marginal AOA p.d.f. in azimuth plane:

$$f_{\phi_b}(\phi_b) = \frac{3D\cos\phi_b}{4a^3}\left(a^2 - D^2\sin^2\phi_b\right) \qquad \sin^{-1}\left(-\frac{a}{D}\right) \le \phi_b \le \sin^{-1}\left(\frac{a}{D}\right). \tag{63}$$

The last solution approach shows that the azimuth angular distribution is independent of b and coincides with equation (56). Hence, we conclude that the limiting equation (56), valid for $b \to 0$, is also true for all b.

Finally, using the closed form expression for the p.d.f. we evaluate the r.m.s angular spread in closed form:

$$\phi_{rms} = 2\phi_{std} \tag{64}$$

where

$$\phi_{std}^2 = \int_{\sin^{-1}\left(-\frac{a}{D}\right)}^{\sin^{-1}\left(\frac{a}{D}\right)} \phi_b^2 f_{\phi_b}(\phi_b) d\phi_b = \left(\sin^{-1}\left(\frac{a}{D}\right)\right)^2 + \frac{2}{3}\sqrt{\frac{D^2}{a^2}-1}\sin^{-1}\left(\frac{a}{D}\right)\left(4-\frac{D^2}{a^2}\right) - \frac{26}{9} + \frac{2}{3}\frac{D^2}{a^2}. \tag{65}$$

G. MARGINAL AOA P.D.F. IN ELEVATION PLANE FOR THE SPHEROID SPATIAL CHANNEL MODEL

As noted in section C of the present chapter, the marginal AOA p.d.f. in elevation plane is given by:

$$f_\beta(\beta) = \frac{1}{V}\int_{\phi_{b_1}(\beta)}^{\phi_{b_2}(\beta)}\int_{r_{b_1}(\phi_b,\beta)}^{r_{b_2}(\phi_b,\beta)} r_b^2 \cos\beta d\phi_b = \frac{1}{3V}\int_{\phi_{b_1}(\beta)}^{\phi_{b_2}(\beta)}\left[r_{b_2}^3(\phi_b,\beta) - r_{b_1}^3(\phi_b,\beta)\right]\cos\beta d\phi_b \tag{66}$$

$$f_\beta(\beta) = \frac{2}{3V}\int_{0}^{\phi_{b_2}(\beta)=\phi_{\max}}\left[r_{b_2}^3(\phi_b,\beta) - r_{b_1}^3(\phi_b,\beta)\right]\cos\beta d\phi_b, \quad |\beta| \le \beta_M \tag{67}$$

The maximum elevation angle β_M is obtained from the values that bound the spheroid in the xz-plane and can be found analytically from the equation (29) by setting the azimuth angle ϕ_b equals to zero:

$$\beta_M = \tan^{-1}\left(\frac{b}{\sqrt{D^2-a^2}}\right). \tag{68}$$

Using the equations (31) through (35), the integral in equation (67) can be simplified as follows:

$$f_\beta(\beta) = \tfrac{2}{3V}\int_0^{\phi_{\max}} \cos\beta\left(r_{b_2} - r_{b_1}\right)\left(r_{b_1}^2 + r_{b_1} r_{b_2} + r_{b_2}^2\right)d\phi_b$$

$$= \tfrac{2\cos\beta}{3V}\int_0^{\phi_{\max}} \tfrac{\sqrt{B^2(\beta)\cos^2\phi_b - 4A(\beta)C}}{A(\beta)}\left(\tfrac{B^2(\beta)\cos^2\phi_b}{A^2(\beta)} - \tfrac{C}{A(\beta)}\right)d\phi_b$$

$$= \tfrac{2B^2(\beta)\cos\beta}{3A^3(\beta)V}\int_0^{\phi_{\max}} \cos^2\phi_b\sqrt{B^2(\beta)\cos^2\phi_b - 4A(\beta)C}\,d\phi_b -$$

$$-\tfrac{2C\cos\beta}{3A^2(\beta)V}\int_0^{\phi_{\max}} \sqrt{B^2(\beta)\cos^2\phi_b - 4A(\beta)C}\,d\phi_b\,. \qquad (69)$$

Substituting the functional forms of $A(\beta)$, $B(\beta)$ and C from equation (26) we get:

$$f_\beta(\beta) = \frac{8D^2b^4\cos^3\beta}{3(a^2\sin^2\beta + b^2\cos^2\beta)^3V}\int_0^{\phi_{\max}} \cos^2\phi_b\sqrt{B^2(\beta)\cos^2\phi_b - 4A(\beta)C}\,d\phi_b -$$

$$-\frac{2b^2\left(D^2 - a^2\right)\cos\beta}{3(a^2\sin^2\beta + b^2\cos^2\beta)^2V}\int_0^{\phi_{\max}} \sqrt{B^2(\beta)\cos^2\phi_b - 4A(\beta)C}\,d\phi_b\,. \qquad (70)$$

The upper limit for the azimuth angle $\phi_{\max}$, for a fixed β, is the largest value of angle ϕ_b that bound the region R, which is generated by the intersection of the cone β = constant with the spheroid. In general, the intersection will include all the points $r_{b_1} \le r_b \le r_{b_2}$, where r_{b_1} and r_{b_2} are given in equation (27). Once again, at the boundary points it yields $r_{b_1} = r_{b_2}$. Thus $\phi_{\max}$ is obtained by setting the discriminant $\Delta(\phi_b) = B^2(\beta)\cos^2\phi_b - 4A(\beta)C$ equals to zero and solving with respect to ϕ_b:

$$\phi_{\max} = \sin^{-1}\left[\tfrac{a}{D}\sqrt{1 - \left(\tfrac{\tan\beta}{\tan\beta_M}\right)^2}\right]. \qquad (71)$$

In order to be able to solve the integral in equation (70) we have to simplify the expression for the discriminant $\Delta(\phi_b) = B^2(\beta)\cos^2\phi_b - 4A(\beta)C$ under the square root. This is done applying the same approach as in previous section D. The discriminant, at a specific value of β becomes equals to zero when the azimuth angle ϕ_b coincides with the maximum value of $\phi_b = \phi_{\max}$. Thus writing the discriminant as

$$\Delta(\phi_b) = \Delta(\phi_b) - \Delta(\phi_{\max})$$

$$= [B^2(\beta)\cos^2\phi_b - 4A(\beta)C] - [B^2(\beta)\cos^2\phi_{\max} - 4A(\beta)C], \text{ becomes}$$

$$\Delta(\phi_b) = \left[4D^2b^4\cos^2\beta\cos^2\phi_b - 4b^2\left(D^2 - a^2\right)\left(a^2\sin^2\beta + b^2\cos^2\beta\right)\right] -$$

$$-\left[4D^2b^4\cos^2\beta\cos^2\phi_{\max} - 4b^2\left(D^2 - a^2\right)\left(a^2\sin^2\beta + b^2\cos^2\beta\right)\right] \tag{72}$$

which gives:

$$\Delta(\phi_b) = \Delta(\phi_b) - \Delta(\phi_{\max}) = 4D^2b^4\cos^2\beta(\sin^2\phi_{\max} - \sin^2\phi_b). \tag{73}$$

Substituting equation (73) into equation (70) gives:

$$f_\beta(\beta) = \frac{16D^3b^6\cos^4\beta}{3(a^2\sin^2\beta + b^2\cos^2\beta)^3V}\int_0^{\phi_{\max}}\cos^2\phi_b\sqrt{(\sin^2\phi_{\max} - \sin^2\phi_b)}d\phi_b -$$

$$-\frac{4Db^4\left(D^2 - a^2\right)\cos^2\beta}{3(a^2\sin^2\beta + b^2\cos^2\beta)^2V}\int_0^{\phi_{\max}}\sqrt{(\sin^2\phi_{\max} - \sin^2\phi_b}\,d\phi_b\,. \tag{74}$$

The above two integrals may be rewritten as:

$$\int_0^{\phi_{\max}}\cos^2\phi_b\sqrt{(\sin^2\phi_{\max} - \sin^2\phi_b)}d\phi_b = \sin\phi_{\max}\int_0^{\phi_{\max}}\cos^2\phi_b\sqrt{(1 - \frac{1}{\sin^2\phi_{\max}}\sin^2\phi_b)}d\phi_b \tag{75}$$

and $$\int_0^{\phi_{\max}}\sqrt{(\sin^2\phi_{\max} - \sin^2\phi_b)}d\phi_b = \sin\phi_{\max}\int_0^{\phi_{\max}}\sqrt{(1 - \frac{1}{\sin^2\phi_{\max}}\sin^2\phi_b)}d\phi_b\,. \tag{76}$$

These integrals can be evaluated in terms of complete elliptical integrals first and second

kind. Indeed with the help of the formulas 2.595-1 and 2.592-2 of [Ref. 5], these integrals take the form:

$$\sin\phi_{\max}\int_0^{\phi_{\max}}\cos^2\phi_b\sqrt{\left(1-\frac{1}{\sin^2\phi_{\max}}\sin^2\phi_b\right)}d\phi_b=\frac{\sin^2\phi_{\max}+1}{3}E(\sin\phi_{\max})-\frac{\sin^2\phi_{\max}-1}{3}K(\sin\phi_{\max}) \tag{77}$$

and

$$\sin\phi_{\max}\int_0^{\phi_{\max}}\sqrt{\left(1-\frac{1}{\sin^2\phi_{\max}}\sin^2\phi_b\right)}d\phi_b=E(\sin\phi_{\max})-\left(\sin^2_{\phi_{\max}}-1\right)K(\sin\phi_{\max}) \tag{78}$$

where $K(\sin\phi_{\max})$ and $E(\sin\phi_{\max})$ denote the complete elliptical integral of the first and second kind respectively [Ref. 5].

Substituting the results from the equations (77) and (78) into equation (74) we get the final expression for the marginal AOA p.d.f., in elevation $f_\beta(\beta)$ in a closed form as follows:

$$f_\beta(\beta)=\frac{16D^3b^6\cos^4\beta}{6(a^2\sin^2\beta+b^2\cos^2\beta)^3V}\left[\left(1+\sin^2\phi_{\max}\right)E(\sin\phi_{\max})-\cos^2\phi_{\max}K(\sin\phi_{\max})\right]-$$

$$-\frac{4Db^4\left(D^2-a^2\right)\cos^2\beta}{3(a^2\sin^2\beta+b^2\cos^2\beta)^2V}\left[E(\sin\phi_{\max})-\cos^2\phi_{\max}K(\sin\phi_{\max})\right],\quad |\beta|\le\beta_M \tag{79}$$

with $\beta_M=\tan^{-1}\left(\frac{b}{\sqrt{D^2-a^2}}\right)$, $\sin\phi_{\max}=\frac{a}{D}\sqrt{1-\left(\frac{\tan\beta}{\tan\beta_M}\right)^2}$ and $V=\frac{4}{3}\pi a^2b$.

III. NUMERICAL RESULTS AND DISCUSSION

Having derived closed form expressions for the marginal AOA p.d.f. in azimuth and elevation planes, we now present in this chapter some numerical results for each marginal AOA p.d.f.. Recall that D is the distance between transmitter and receiver, a is the semi-major axis of the spheroid, and b is the semi-minor-axis of the spheroid.

A. PLOTS FOR MARGINAL AOA PDF IN AZIMUTH PLANE

In this section we consider the cases of 'D', 'a' and 'b' as given in Table 2 and generate some plots:

D(m)	a (m)	b(m)	Corresponding Figure
1000	100	0.001	10
1000	100	50	11
1000	200	150	12

Table 2. Parameters of D, a and b used in plots for marginal AOA p.d.f. in the azimuth plane.

Figure 10 has been plotted in order to check how the azimuth angular distributions of the spheroid and the circular scattering models are related to each other. The circular scattering model is presented in [Ref. 3]. The angular distribution for the circular model is given by equation (80):

$$f_{\phi_b}(\phi_b) = \begin{cases} \frac{2D\cos\phi_b\sqrt{D^2\cos^2\phi_b - D^2 + a^2}}{\pi a^2}, \sin^{-1}\left(-\frac{a}{D}\right) \le \phi_b \le \sin^{-1}\left(\frac{a}{D}\right) \\ 0, else \end{cases} \quad (80)$$

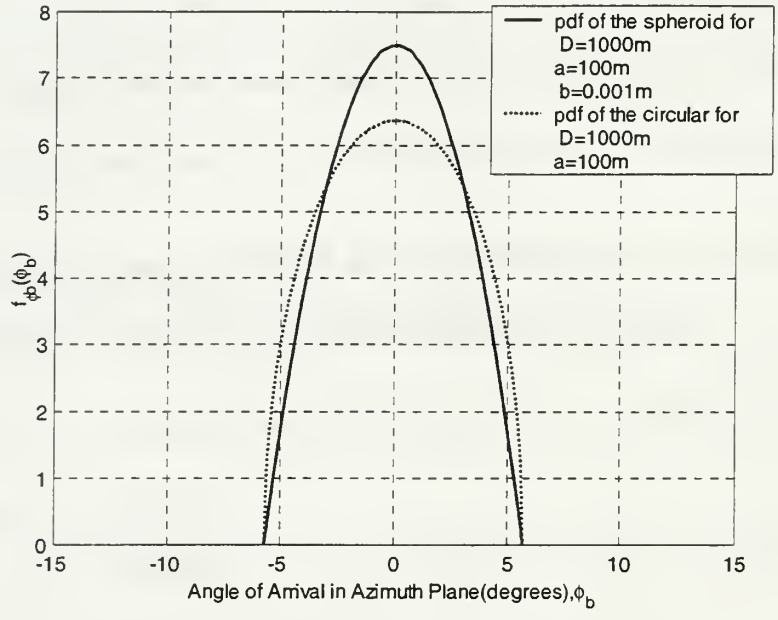

Figure 10. Plot of $f_{\phi_b}(\phi_b)$ versus ϕ_b for D=1000m, a=100m and b=0.001m. Also shows the AOA p.d.f. for a circular spatial model for D=1000m and a=100m.

In Figure 10, we plot the p.d.f. for a/D=0.1 and b/D=10^{-6}. Comparing the plot of the spheroid model for small values of 'b' with this of the circular model, we can observe that there exists a significant difference between them.

In Figures 11 and 12 we plot the p.d.f. for a/D=0.1, b=50m and for a/D=0.2, b=150m using the two different formulas for the angular distribution in the azimuth plane.

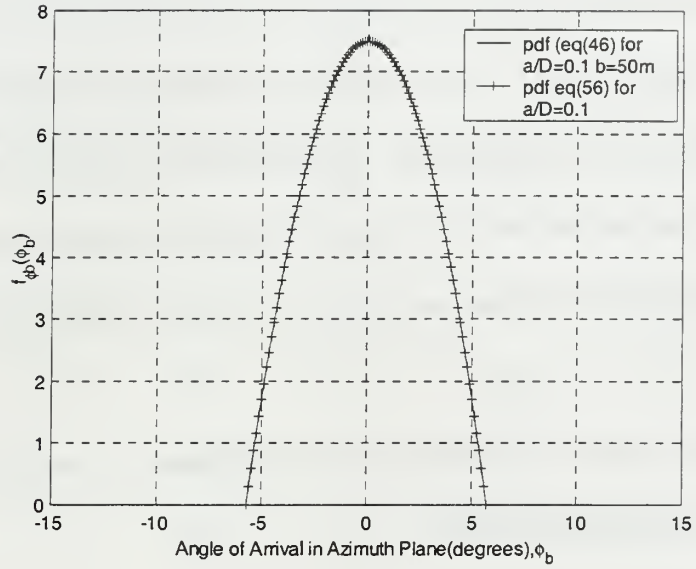

Figure 11. Plot of $f_{\phi_b}(\phi_b)$ versus ϕ_b for D=1000m, a=100m and b=50m (using the two different formulas).

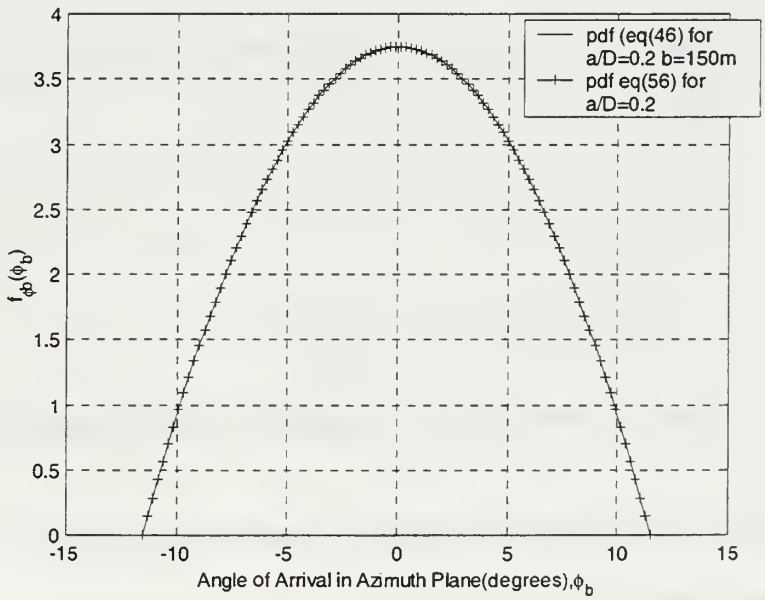

Figure 12. Plot of $f_{\phi_b}(\phi_b)$ versus ϕ_b for D=1000m, a=200m and b=150m (using the two different formulas).

As shown Figure 11 and 12, the two different formulas give identical results for the angular distribution in azimuth plane. Additionally, we conclude that the higher the ratio *a/D*, the lower the probability for the received signals at the base station to be restricted in a small angular region centered about the axis which connects the base and the mobile stations.

Finally in Figure 13 we plot the r.m.s angle spread in azimuth plane as given in equation (64) versus the ratio *a/D*.

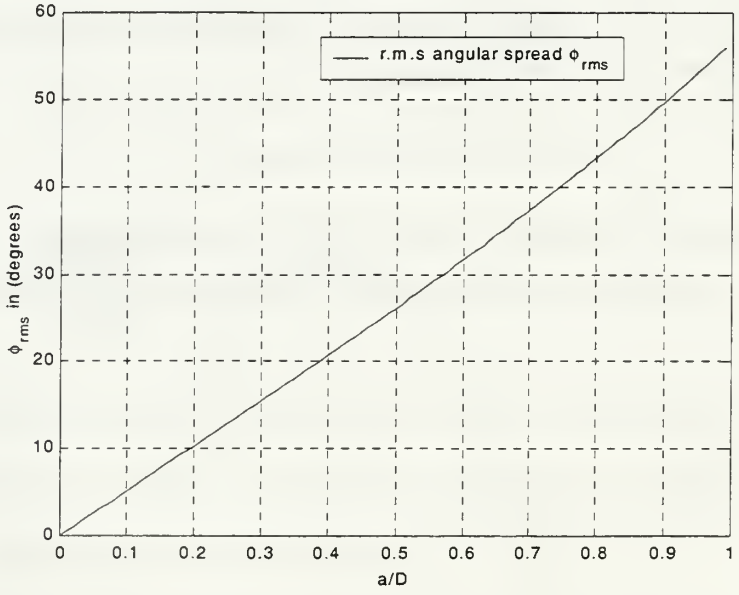

Figure 13. Plot of the r.m.s angular ϕ_{rms} spread versus a/D.

Figure 13 shows that for values up to 0.5, of the ratio *a/D*, the profile of the r.m.s angle spread is almost linear. Note that the r.m.s angle spread in azimuth plane is independent of *b* as proved with the derivation of the second formula for the p.d.f in azimuth plane.

B. PLOTS FOR MARGINAL AOA PDF IN ELEVATION PLANE

D(m)	a(m)	b(m)	Corresponding Figure
1000	100	1	14
1000	100	30	15
1000	100	50	16
1000	200	50	17
1000	500	50	18

Table 3. Parameters *D*, *a*, and *b* used in plots for marginal AOA p.d.f. in the elevation plane.

Figure 14 is generated to demonstrate the angular distribution in elevation plane for small values of *b*.

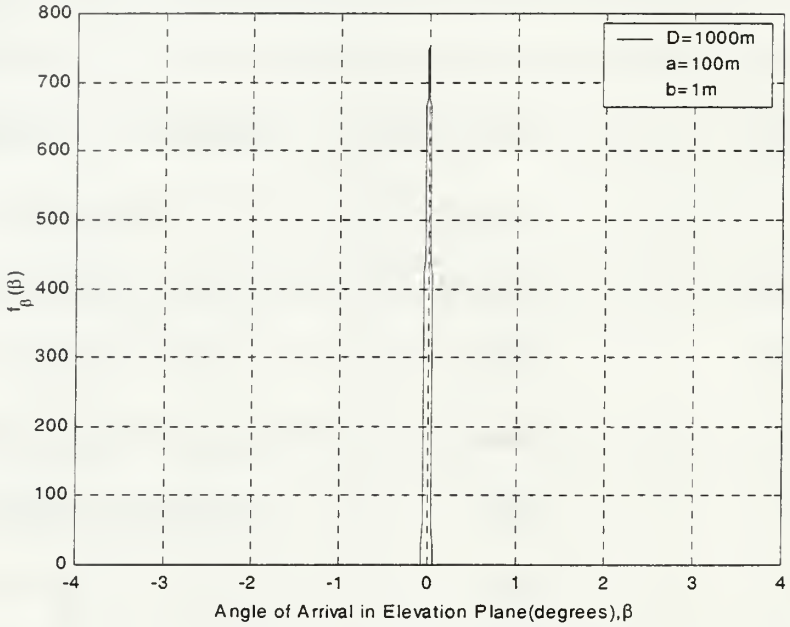

Figure 14. Plot of $f_\beta(\beta)$ versus β for D=1000m, a=100m and b=1m..

As we can see form the Figure 14 the angular distribution in elevation plane for small values of b looks like a dirac function as it is expected.

Figure 15 and 16 are plotted for demonstration purposes, giving information of how the changes of the ratio *b/D* for a given 'a' affect the angular distribution in elevation plane.

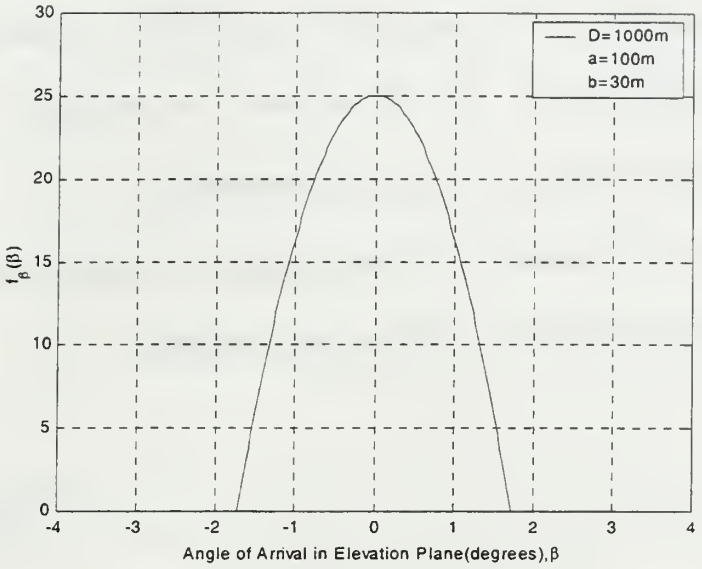

Figure 15. Plot of $f_\beta(\beta)$ versus β for D=1000m, a=100m and b=30m..

Figure 15 shows the the angular distribution in elevation plane for a ratio *b/D*=0.03 and *a/D*=0.1.

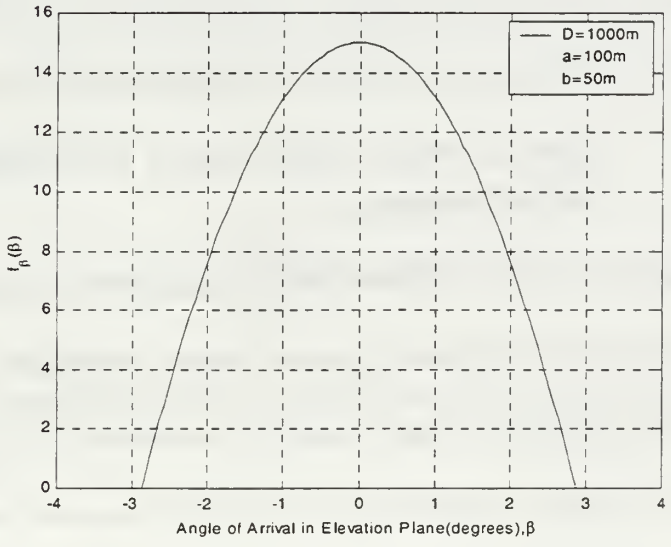

Figure 16. Plot of $f_\beta(\beta)$ versus β for D=1000m, a=100m and b=50m.

Figure 16 shows the p.d.f for a ratio *b/D*=0.05 and *a/D*=0.1 As seen, compared to Figures 15 and 16, the higher the ratio *b/D* the lower the probability to receive multipath components from a small region β_{BW} at the base station.

Figure 17 is generated, as set with Figure 16, in order to show the effect of the length of the semi- major axis a on the angular distribution.

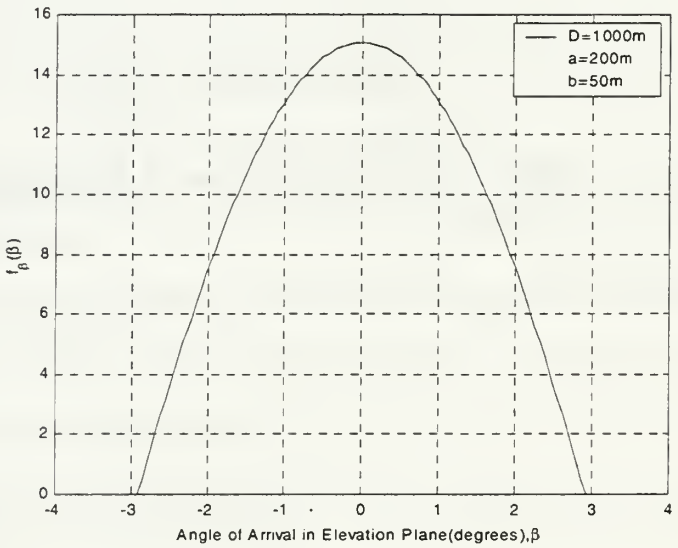

Figure 17. Plot of $f_{\beta}(\beta)$ versus β for D=1000m, a=200m and b=50in meters.

Figure 17 shows the p.d.f for a ratio *b/D*=0.05 and *a/D*=0.2. Comparing Figures16 and 17, it is seen that p.d.f in elevation plane is almost independent of the length of semi-major axis of the spheroid for small values of the ratio *a/D*. Figure 18, is generated to show the effect of higher values of the *a/D* ratio on the angular distribution.

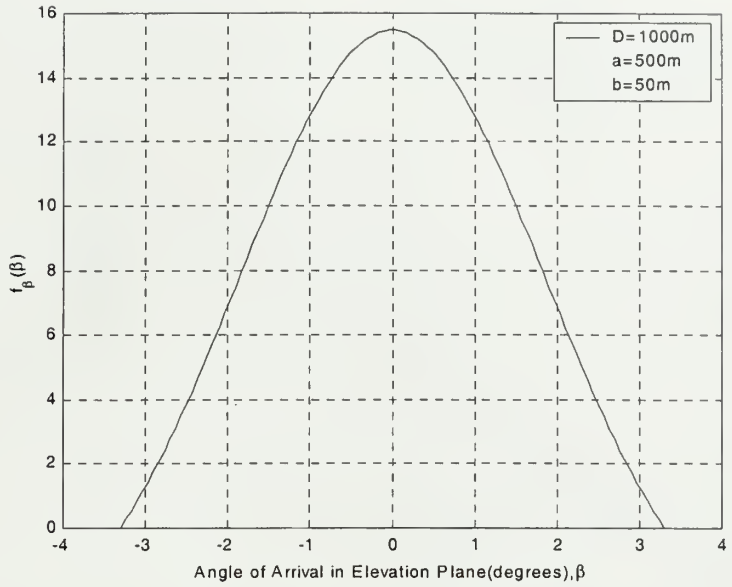

Figure 18. Plot of $f_\beta(\beta)$ versus β for D=1000m, a=500m, and b=50m.

Comparing Figure 17 and 18, it was observed that there exists a difference between the two angular distributions.

Finally in Figure 19 we plot the r.m.s angular spread of the angle of arrival in elevation plane, as given by the equation (81), versus the ratio b/D for specific values of *a/D*.

$$\beta_{rms} = 2\sqrt{\int_{-\frac{\pi}{2}}^{\frac{\pi}{2}} \beta^2 f_\beta(\beta) d\beta} \tag{81}$$

The mean value of the angular distribution at the base station is zero, and the integral is evaluated numerically.

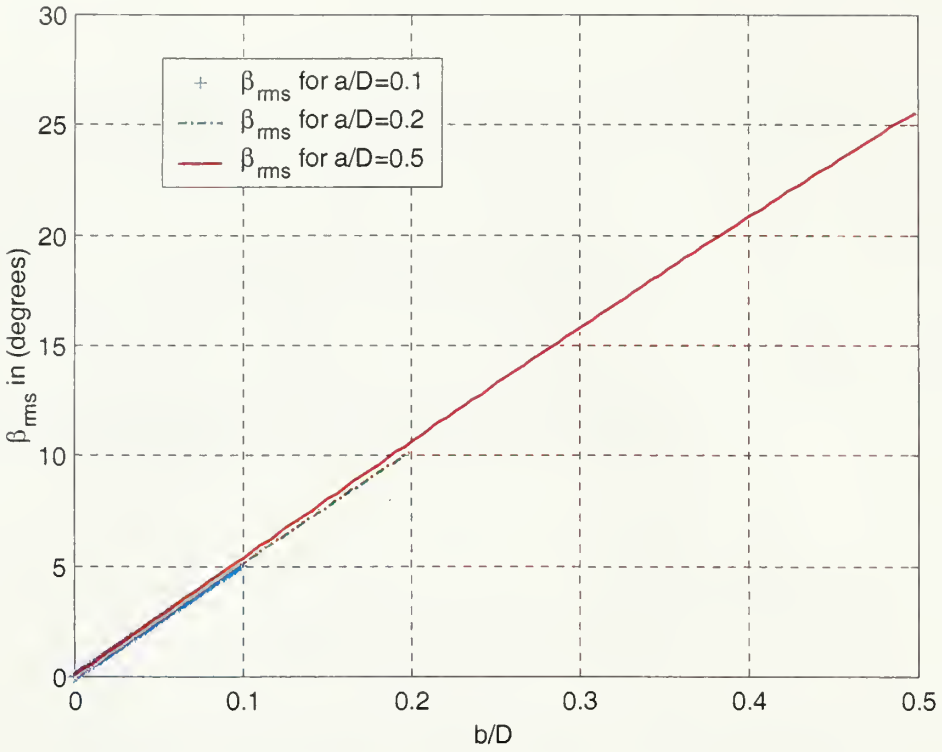

Figure 19. Plot of the r.m.s angular β_{rms} spread versus b/D for various ratios a/D,for the spheroid scattering model.

As shown in Figure 19, there exists a linear relation between the r.m.s angular spread and the ratio b/D independently of the ratio a/D.

Eventually for validation purposes of the two derived, in this thesis, closed forms of the angular distributions, we plot in Figure 20 both p.d.f. with *a* almost equals to *b* (*b* is not made exactly equal to *a* to avoid dealing with limiting process).

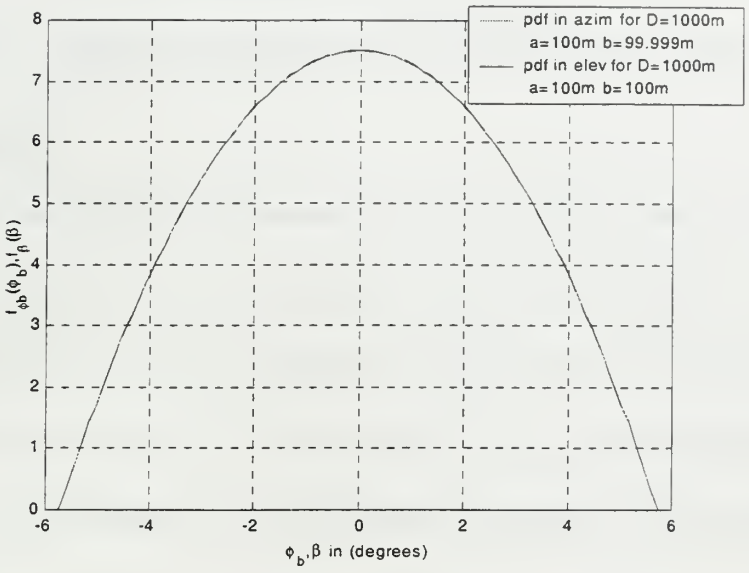

Figure 20. Plot of $f_{\phi_b}(\phi_b)$ versus ϕ_b and $f_\beta(\beta)$ versus β for D=1000m, a=100m and b=99.99m and for D=1000m, a=100m and b=100m respectively.

Figure 20, shows the angular distribution in azimuth and elevation plane for *a/D=b/D*=0.1. From the plot we can see identical results for both angular distributions, as expected due to the symmetry of the model.

THIS PAGE INTENTIONALLY LEFT BLANK

IV. CONCLUSIONS AND RECOMMENDATIONS

A. CONCLUSIONS

In this thesis we proposed a geometrically based single bounce scattering 3D model. It has been assumed that the scatterers are distributed about the mobile with a constant density function in a volume as defined by the geometry of the spheroid. The distance between the base station and the mobile station is D. The focus of the effort of this research was in the derivation of the mathematical expressions which described the spatial statistics properties of the received signals in the presence of the three-dimensional multipath scattering.

After presenting a general approach for the derivation of the joint TOA/AOA and marginal AOA p.d.f.s in terms of an arbitary scatterer probability density function, we presented the derivation of the angular distribution in azimuth and elevation plane for the spheroidal model in closed expression forms.

Making use of these quantities we studied the behavior of the angular spread for each p.d.f as function either of the spheroid dimensions or of the distance between the transmitter and the receiver. For either angular distribution the model results in a higher probability of arrival along the line of sight direction. Also, we observed that the higher the ratio of each spheroid's dimension over the distance D the lower the probability that the multipath components are confined to a small region. An excellent agreement exists in the plots which are generated from the two different formulas of the p.d.f in azimuth plane.

Analytical and numerical calculations were performed for the r.m.s angular spread in azimuth and elevation planes respectively. The effect of the ratio a/D or b/D on the corresponding angular spread was investigated.

B. RECOMMENDATIONS

Further research is required to enhance this model. It will be a interesting to derive the marginal time of arrival p.d.f or to investigate the effect of the angular spread on the correlation observed between the received signals an antenna array. Another area of interest should be the validation of this model. This could be done comparing with measurements taken over similar macrocell environments.

LIST OF REFERENCES

1. Janaswamy, R., *Radiowave Propagation and Smart Antennas for Wireless Communications*, Kluwer Academic Press, 2000.

2. Ertel, R.B., Cardieri, P., Sowerby, K.W., Rappaport, T.S., and Reed, J.H., "Overwiew of Spatial Channel Models for Antenna Array Communication Systems," *IEEE Personal Communications., pp. 10-22, February 1998.*

3. Ertel, R.B. and Reed, J.H., "Angle and Time of Arrival Statistics for Circular and Elliptical Scattering Models,"*IEEE Journal on Selected Areas in Communications.,* vol. 17(11), pp. 1829-1840, November 1999.

4. Papoulis,A, *Probability, Random Variables, and Stochastic Processes,* 3rd ed., McCraw-Hill Book Co., 1991.

5. Gradshteyn, I.S. and Ryzhik, I.M., *Table of Integrals, Series, and Products,* 5th ed., Academic Press, 1994.

6. Liberti, J.C., and Rappaport, T.S., *Smart Antennas for Wireless Communications,* 1st ed., Prentice Hall, Inc, 1999.

THIS PAGE INTENTIONALLY LEFT BLANK

INITIAL DISTRIBUTION LIST

1. Defense Technical Information Center 2
   8725 John J. Kingman Road, Suite 0944
   Ft. Belvoir, VA 22060-6218

2. Dudley Knox Library 2
   Naval Postgraduate School
   411 Dyer Road
   Monterey, CA 93943-5101

3. Chairman, Code EC.....1
   Department of Electrical and Computer Engineering
   Naval Postgraduate School
   Monterey, CA 93943-5121

4. Professor Ramakrishna Janaswamy, Code EC/Js.....3
   Department of Electrical and Computer Engineering
   Naval Postgraduate School
   Monterey, CA 93943-5121

5. Professor Tri Ha, Code EC/Ha.....1
   Department of Electrical and Computer Engineering
   Naval Postgraduate School
   Monterey, CA 93943-5121

6. LT. Christos Sasiakos.....3
   13 Dabaki Street
   11526 E. Stavros
   Athens, Greece